Canadian
Journal of Technology

A DISTILLATION METHOD FOR THE SEPARATION OF IMPURITIES IN COMMERCIAL CHLORINE[1]

BY F. W. MATTHEWS AND G. G. WARREN

ABSTRACT

An apparatus is described whereby the impurities in a 10 liter sample of liquid chlorine are concentrated and separated into three fractions for further analysis. Distillation at normal pressure was carried out in two all-glass laboratory columns using glass helices packing and reflux control. The residue after removal of the chlorine was fractionated by simple vacuum distillation and sublimation.

INTRODUCTION

Chlorine manufactured by the electrolysis of sodium chloride brine normally contains small amounts of organic impurities which become evident when very large quantities are evaporated in industrial processes. These impurities are present in low concentration (10 to 500 p.p.m.) hence they are difficult to separate and identify.

This paper describes a distillation scheme which concentrates the impurities from 10 liters (35 lb.) of liquid chlorine and separates the impurities into fractions according to their vapor pressures. Hedgepath and Riggs (1) described an unpacked column without reflux control for the distillation of chlorine. Their design was modified and used as a starting point in the present work.

DESCRIPTION OF THE STILLS

The stills (Fig. 1) are designed to reduce a sample of about 10 liters of liquid chlorine in two stages to a convenient sample containing only those materials in the chlorine which boil above the boiling point of liquid chlorine at atmospheric pressure ($-34°C.$). Stage I consists of a 12 liter flask, a silvered dewar jacketed 5 plate column packed with 1/8 in. glass helices, a vapor take-off with solenoid operated fractionator, and a $-60°C.$ reflux condenser. Stage II, to which the sample is transferred after reduction to less than 500 ml., consists of a 0.5 liter flask, a silvered dewar jacketed column packed with 1/8 in. glass helices, a liquid take-off with solenoid operated fractionator, and a $-60°C.$ reflux condenser. The final sample, essentially chlorine-free and containing the less volatile impurities, may then be weighed and is ready for further analyses.
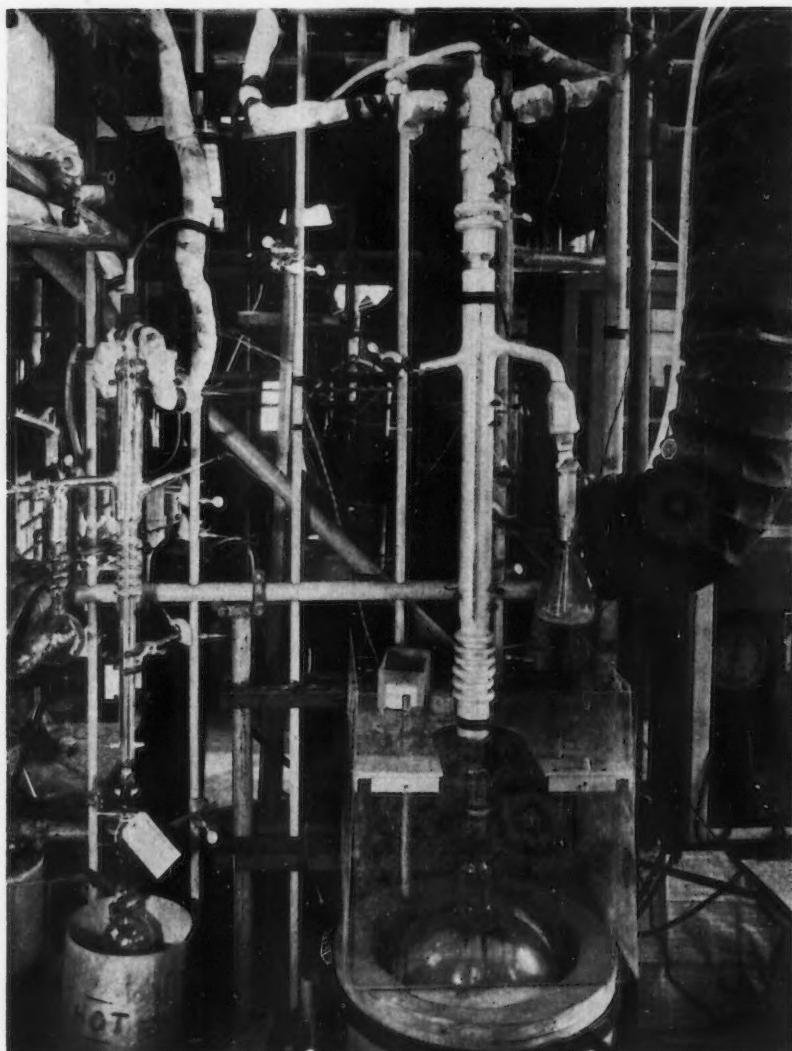
FIG. 1.   Photograph of distillation apparatus for separation of impurities from chlorine.

Appended to the stills are a cooling system for the condensers and a control-panel. The cooling system circulates methanol cooled by dry-ice (CO_2) to about $-60°C$. through the reflux condensers of each still, using 7 g.p.m. centrifugal pumps. Thermocouples are attached to the coolant lines at the inlet and outlet of the condensers to assure proper operation.

When handling a large quantity of poisonous gas special safety precautions are required. The still is set up in a laboratory equipped with special exhaust
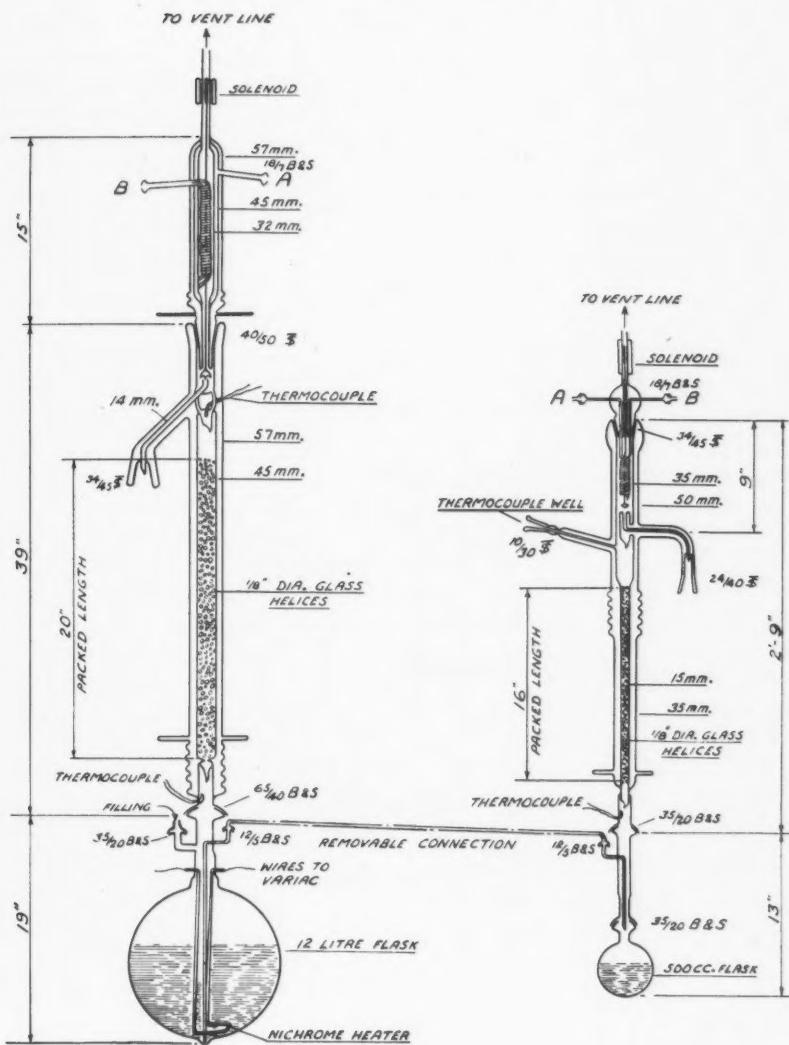
FIG. 2. Drawing of distillation apparatus for separation of impurities from chlorine.

fans which were fitted with flexible ducts leading to the still-pots and condenser heads. The large (Stage I) flask containing 35 lb. of chlorine is supported on a spring-loaded platform which avoids strains on the glassware. The internal glass enclosed heating element was chosen for the large flask as it provided excellent control and at the same time greater safety in case of breakage of the distillation flask.

OPERATIONS

The Stage I still-pot is filled through the filling sidearm by a suitable line either from a cylinder or other source of chlorine after passage through a cooling coil immersed in dry-ice/methanol. The chlorine is thus precooled to below its boiling point ($-34°C$.), the still-pot is also precooled, and the still-head is at total reflux. After the still-pot is filled, the insulated can used to hold dry-ice is lowered and the electric heater started. When the packed column becomes thoroughly wet, the take-off may be operated. Reduction from
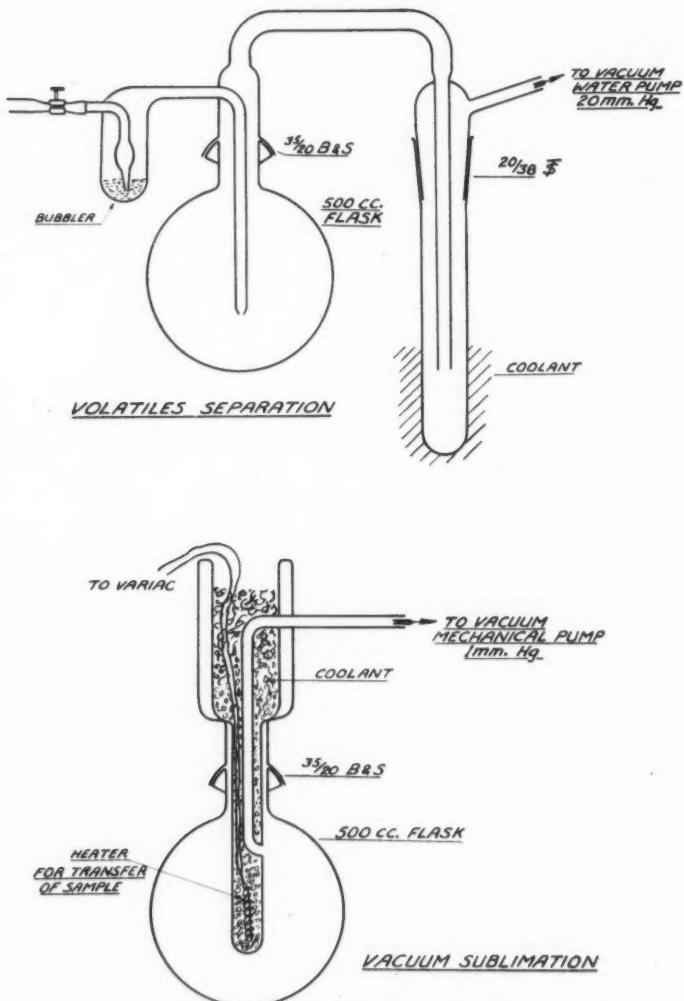
Fig. 3. Drawing of apparatus for fractionation of impurities.

10,000 ml. to less than 500 ml. takes four to six hours when the vapor take-off is open for eight seconds and the reflux two seconds. After both flasks have been cooled with dry-ice, the transfer to the smaller still-pot is accomplished by connecting the transfer line and applying a gentle suction to the small flask, thus pulling the chlorine into the Stage II still-pot.

The 500 ml. sample is then reduced without heating on the Stage II still using a 1:1 reflux ratio until the flask approaches room temperature. This also requires four to six hours. If red bands of bromine containing hydrocarbon appear in the packing they can be returned by cooling the still-pot with dry-ice.

At the beginning, about 40 lb. of crushed dry-ice and 3 gal. of methanol are required as a coolant for the circulating alcohol. A further 40 lb. dry-ice are required for a six hour run of the stills. When not in use all openings to the stills are either capped with solid stoppers or calcium chloride drying tubes.

The apparatus was attended by two men wearing gas masks during any transfer of chlorine. At other times the stills were sufficiently automatic to require only occasional attention.

STAGE III OPERATIONS

The residue in the still-pot from the Stage II distillation is first separated into two fractions. After the flask has been connected to a cold trap surrounded by dry-ice and methanol, with a slight air current sweeping through, it is allowed to come to room temperature to remove the chlorine. No indication of methyl chloride (boiling point $-21°C.$) was found in this work. A water pump vacuum (20 mm. Hg) is then applied and the volatile liquids are distilled over to the trap (Fig. 3). This results in a separation into a volatile liquid "A" and a less volatile "solid" fraction.

The flask containing the "solid" fraction is placed under a cold finger and vacuum applied (1 mm. Hg). Sublimation occurs which is aided by applying hot water 70°C. to the outside of the flask. The resulting fractions, the sublimate containing the volatile solids ("B"), and the final residue ("C") are weighed and sent for further analysis if required.

The second and third stage separations may have to be modified to yield more or different fractions depending on the nature of the impurities. For instance, we have found chlorine in which fractions "B" and "C" are high boiling liquids and from which no solid fractions were separated.

RESULTS

In this apparatus we have distilled samples of chlorine from five commercial sources and separated impurities which were later determined by infrared absorption, mass spectrometry, or X-ray diffraction. Some of the compounds identified were methylene chloride, chloroform, carbon tetrachloride, hexachloroethane, and hexachlorobenzene (see Table I).

When operated in daylight there is the probability of a reaction between the chlorine and hydrogen containing hydrocarbons. This was observed when a quantity of methylene chloride was added to redistilled chlorine and there

TABLE I

Commercial chlorine sample 10 liters	$\longrightarrow$	Total impurities 3 to 40 ml. 300 to 4000 p.p.m.		

Fraction "A" 220 to 3700 p.p.m.	+	Fraction "B" 5 to 350 p.p.m.	+	Fraction "C" 5 to 230 p.p.m.
CCl_4, $CHCl_3$ CH_2Cl_2, Br, etc.		C_2Cl_6, etc.		C_6Cl_6 $FeCl_3$, etc.
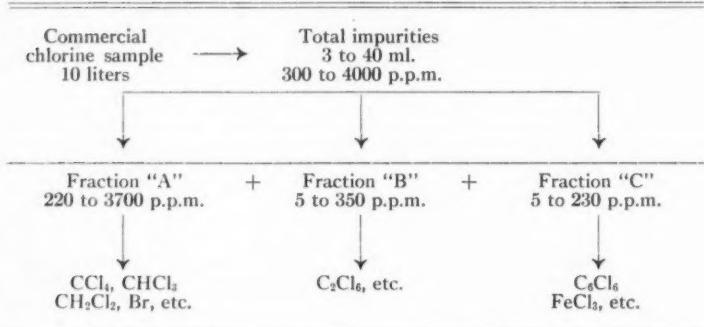
was recovered by distillation an equivalent mixture of chloroform and carbon tetrachloride. When monochlorobenzene was added, a material tentatively identified as octachlorocyclohexane was recovered. To lessen these reactions catalyzed by light, the stills were blacked out by taping all clear glass parts but no actual comparisons were made to test the effectiveness of this change.

REFERENCE

1. HEDGEPATH, L. L. and RIGGS, W. S. J. Am. Water Works Assoc. 30: 1671. 1938.

AN INSTRUMENT FOR LEAK DETECTION AND PRESSURE MEASUREMENT IN HIGH VACUUM SYSTEMS[1]

By Edouard G. Leger[2]

ABSTRACT

An instrument is described for measuring gas pressure in the range 10^{-1} to 10^{-7} mm. of mercury. At the higher pressures vacuum thermocouples are used and at the lower pressures ionization gauges. Leaks are detected by spraying oxygen on the outside of the vacuum system and noting the decrease in electrons from a tungsten filament emitter in an ionization gauge when it is operated as a saturated diode. Leaks are traced either by observing a meter or by means of the change in frequency of an audio-oscillator. To avoid damage an automatic cutoff is used to turn off the gauges and diffusion pumps when the pressure reaches a predetermined value.

INTRODUCTION

During the development of a rapid-scanning mass spectroscope for the study of cool flames (5) considerable difficulty was experienced with leaks in the metal vacuum system. There was need for a sensitive instrument for leak detection which would also serve as an apparatus for measuring and monitoring gas pressure. Since an instrument meeting the requirements was not available and none was described in the literature, it was necessary to design and construct one using established circuits and techniques.

The best equipment and welding techniques were used in an effort to prevent leaks in the system but even with these precautions it is difficult to avoid leaks entirely. A leak at the rate of one cubic centimeter per year at a pressure slightly below atmospheric increases to one liter per second at an internal pressure of 10^{-6} mm. of mercury.

It was desirable to operate the high vacuum system continuously for the following reasons:

(a) No time is lost in pumping;

(b) No gassing occurs so that repeated heating is eliminated;

(c) Risk of fatigue fracture of welded joints caused by repeated evacuation of a non-symmetrical system is eliminated.

For continuous operation it was necessary to introduce an automatic device which will turn off the ionization gauges and diffusion pumps when the pressure exceeds a predetermined limit. This requires that the pressure in the system be continuously monitored. In the instrument described two vacuum systems can be connected permanently but monitoring and leak detection can only be accomplished in one system at a time.

PRINCIPLES OF OPERATION

Since measurement of pressures in the range 10^{-1} to 10^{-7} mm. of mercury was required, it was necessary to use two types of detection element. The ionization gauge was used in the high vacuum region of 10^{-3} to 10^{-7} mm. of mercury for measurement of pressure and for leak detection. The gauge has the form of a glass envelope which is incorporated into the system and contains a heated tungsten filament, a grid at positive potential, and an outer plate at negative potential. The electrons which are emitted from the filament ionize the gas in the space between the grid and filament and the ions are attracted to the outer plate. The ionic current to the outer plate is proportional to the gas pressure between the filament and grid and thus to the gas pressure in the system. The circuits required are somewhat complicated if operation from a-c. lines is desired but the gauge is reliable for gas pressure measurements and can also be used for leak detection as described below. For vacuum measuring it is being replaced by Philips gauges.

Ionization gauges cannot be used when the pressure rises above 10^{-3} mm. of mercury without risk of burning out the filament. It was therefore necessary to incorporate a more rugged device into the system to ensure that the pressure is low enough before the ionization gauge is put into operation and for leak detection at pressures in the range 10^{-1} to 10^{-3} mm. of mercury. The vacuum thermocouple was used for this purpose. It consists of a small electrically heated wire to which is soldered a small thermocouple, the whole being mounted in a glass envelope. The temperature of the wire carrying a fixed current depends on the thermal conductivity of the air in the envelope and consequently on the gas pressure. The latter can be obtained from the thermocouple output by means of a calibration curve.

Leak detection at low pressures is accomplished by means of the ionization gauge as described by Dushman (3, p. 372). The method is based on the fact that the emission of a saturated diode with a tungsten filament is easily poisoned by a trace of oxygen. When the outside of the vacuum system is sprayed with oxygen, the increase in concentration of oxygen inside the system caused by the leak reduces the emission of the filament and the effect is indicated on a meter in the grid circuit of the ionization gauge or by means of an audible signal.

CIRCUIT OPERATION

A block diagram of the system is shown in Fig. 1 and the complete circuit diagram in Fig. 2.

The Thermocouple Circuit

The thermocouple circuit is entirely independent of the ionization gauge circuit. It consists of a line-operated low tension power supply and associated control and measuring circuits identical with those found in the CENCO vacuum thermocouple control unit (2) except for one or two minor modifications. A microammeter (0–200) of low internal resistance (M_1) is used to measure both the thermocouple e.m.f. and, by means of a shunt, the current
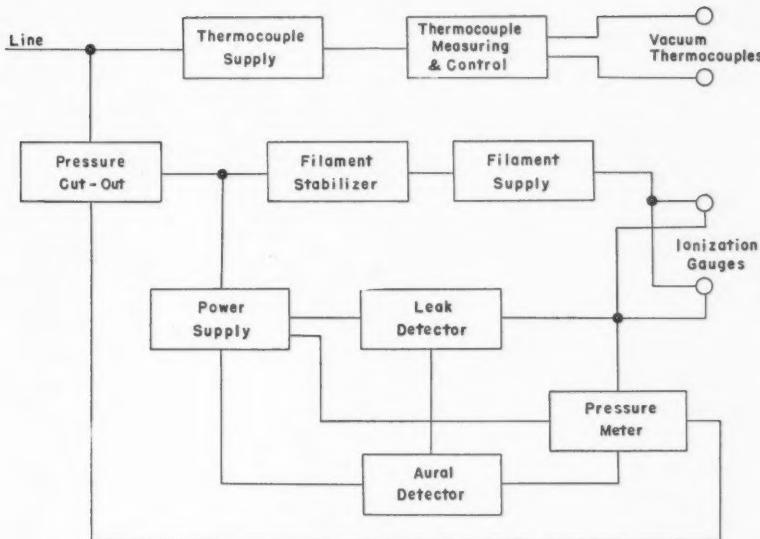
FIG. 1.

in the heating wire. The latter can be adjusted by variable resistors. A switch enables either measuring head V_{10} or V_{14} to be used. The low-tension power is supplied by a transformer T_2 and a full wave selenium rectifier SR.

The Ionization Gauge Circuit

The gauges used are RCA Type 1949. Switch S_{10} allows either of the gauges V_{11} or V_{15} to be selected for use and the switches S_{11} and S_{15} permit operation of either of the filaments in each tube. Since the electron emission from the filament varies with the current through the filament, it is desirable to provide automatic control of the current if the gauge is to be used continuously. The current is controlled by varying the load on a transformer T_1, placed in series with the filament transformer T_3, by means of a thyratron V_1, the grid potential of which is controlled by the grid current through the gauges (7). When the gauges are used for leak detection, the reference potential supplied to the thyratron is controlled by the current through the saturated diode V_4 which has filament characteristics similar to the ionization gauges. Since both the reference tube V_4 and the gauges operate from a stabilized filament supply, variations in gauge filament emission caused by oxygen poisoning can be detected by fluctuations in grid current indicated on the meter M_2. The alternative methods of operation are selected by the switch S_6. The filament current for the reference diode is supplied by a transformer T_4 in parallel with T_3 and also controlled by the thyratron circuit.

When measuring the gas pressure, the grid current through the gauge is adjusted to 10 ma., as shown on the meter M_2, by adjusting the filament
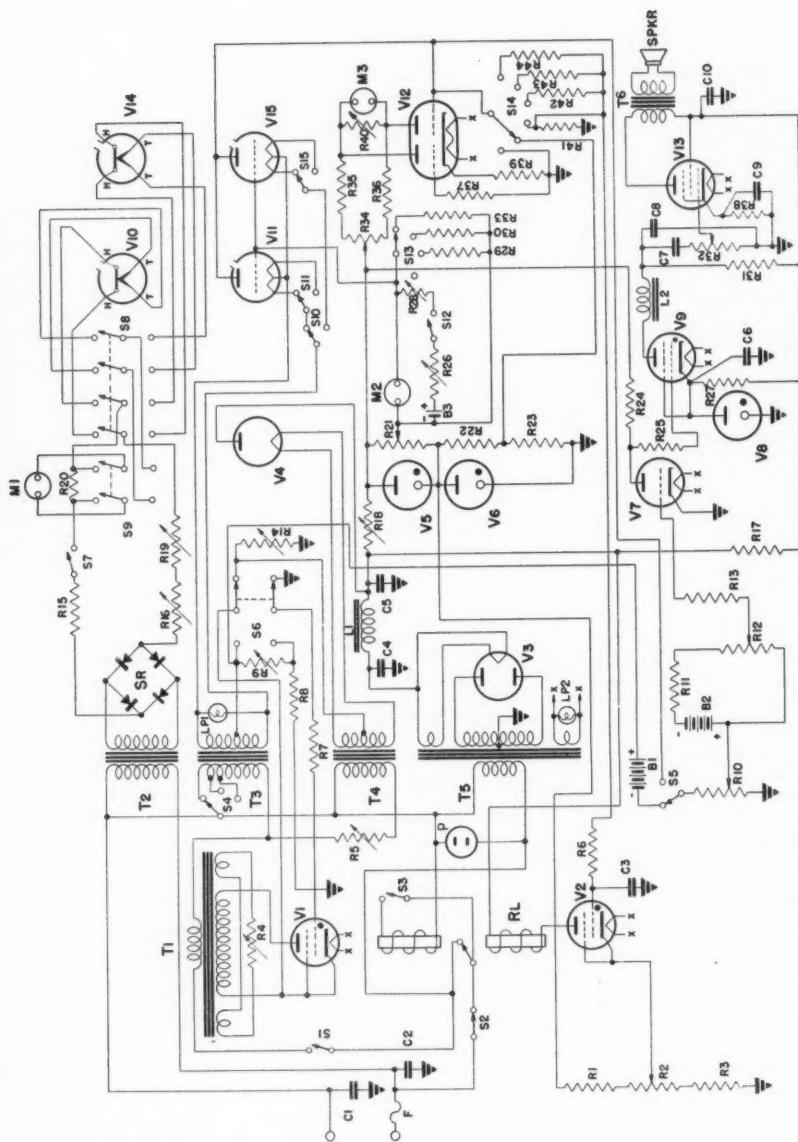
Fig. 2.   An instrument for leak detection and pressure measurement in high vacuum systems.

emission with the resistor R_9. If the current is still insufficient, it can be adjusted by the load R_4 on the transformer T_1 or by changing the tapping S_4 on the transformer T_3. To obtain 10-fold variations in sensitivity it was necessary to fix the filament potential at 22.5 volts above ground by means of R_8 and R_9 and the grid potential at 122.5 volts above ground by means of R_{21}. The plate is connected to ground through the loads R_{41} to R_{44} selected by the switch S_{14}. The potential developed across the load is measured by means of the vacuum-tube voltmeter consisting of twin triode V_{12} and meter M_3 (3, p. 362). The meter zero and maximum are adjusted by means of the variable resistors R_{34} and R_{40} with S_{14} in positions 1 and 2, respectively. When the above adjustments were made and with a meter reading 0–10, the readings were directly in pressure in mm. of mercury $\times 10^{-3}$, $\times 10^{-4}$, $\times 10^{-5}$, and 10^{-6} with the switch S_{14} in positions 3 to 6, respectively. The potential developed across R_{41} is applied to the grid of the thyratron V_2, the sensitivity of which is adjusted so that it fires when the pressure rises to 10^{-3} mm. The filter consisting of R_6 and C_3 prevents the firing of the thyratron by rapid fluctuations in the system. When the thyratron fires, the overload relay RL is energized and the diffusion pump and power supply to the ionization gauges are turned off and remain off until reset by the switch S_3.

When detecting leaks, the gauge filament emission is controlled by the diode V_4, the emission current range being adjusted by R_5. The grid current of the ionization gauge is adjusted to about 10 ma. by varying R_{14}. This current is then nullified by B_3 and R_{26} and the sensitivity of the meter adjusted by S_{13}. Leaks are detected by changes in the meter reading when oxygen is sprayed onto the vacuum system.

PARTS LIST FOR FIG. 2.

C_1, C_2, C_6: 0.1 µf., 600 v. C_3: 0.05 µf., 600 v. C_4, C_5: 32 µf, 450 v. C_7: 0.005 µf., 600 v. C_8: 0.004 µf., 600 v. C_9: 25 µf., 25 v. C_{10}: 8 µf., 500 v.
R_1, R_7, R_{25}: 100 kΩ, 2 w. R_2: 3 kΩ, 2 w. pot. R_3, R_{39}: 2 kΩ, 2 w. R_4: 50 Ω, 10 w. R_5: 50 Ω, 25 w. R_6, R_{13}, R_{37}: 2.2 megs, 2 w. R_8: 17 kΩ, 2 w. R_9, R_{14}, R_{34}: 5 kΩ, 2. w. pot. R_{10}: 5 megs, 2 w. pot. R_{11}: 5 megs, 2 w. R_{12}: 2 megs, 2 w. pot. R_{15}: 50 Ω, 2 w. R_{16}: 30 Ω, 2 w. pot. R_{17}: 10 kΩ, 10 w. R_{18}: 3 kΩ, 10 w. adjustable. R_{19}: 2 Ω, 2 w. pot. R_{21}: 5 kΩ, 10 w. adjustable. R_{22}: 20 kΩ, 2 w. R_{23}: 38 Ω, 2 w. R_{24}: 200 kΩ, 2 w. R_{26}: 40 Ω, 2 w. pot. R_{27}: 400 kΩ, 2 w. R_{28}: 200 Ω, 2 w. adjustable. R_{31}: 500 kΩ, 2 w. R_{32}: 250 kΩ, 2 w. pot. R_{33}, R_{36}: 10 kΩ, 2 w. R_{38}: 500 Ω, 2 w. R_{40}: 25 kΩ, 2 w. pot. R_{41}: 2 kΩ, 1/2 w. 1% Nobleloy. R_{42}: 18 kΩ, 1/2 w. 1% Nobleloy. R_{43}: 198 kΩ, 1/2 w. 1% Nobleloy. R_{44}: 2 megs, 1/2 w. 1% Nobleloy. R_{20}: meter shunt 200 µa. to 100 ma. R_{29}: meter shunt 20 µa. to 200 µa. R_{30}: meter shunt 20 µa. to 2 ma. R_{33}: meter shunt 20 µa. to 20 ma.
T_1: power trans. 300–0–300 v., 70 ma. 5 v. 2 amp. 6.3 v. 2.4 amp. T_2: fil. trans. 6.3 v. 0.3 amp. T_3: fil. trans. 5, 6.3, 7.5 v. ct 6.5 amp. T_4: fil. trans. 5 v. 6 amp. T_5: power trans. 350–0–350 v. 95 ma., 5 v. 2 amp. 6.3 v. 4 amp. T_6: output trans. 6F6 to v.c.
M_1: 0–200 µa. meter, 55 Ω int. resistance. M_2: 0–20 µa. meter. M_3: 0–50 µa. meter.
V_1, V_2, V_9: 2050. V_3: 5U4. V_4: 2V3. V_5: 0D3. V_6: 0C3. V_7: 6J5. V_8: 1/4 w. neon. V_{10}, V_{14}: RCA 1949. V_{11}, V_{15}: RCA 1946. V_{12}: 6SC7. V_{13}: 6F6.
S_1, S_2, S_{12}: SPST. S_3: SPST push button. S_4: SP3T. S_{13}: SP4T. S_5, S_{10}, S_{11}, S_{15}: SPDT. S_6, S_9: DPDT. S_7: SPST on pot. R_{16}. S_8: 4PDT. S_{14}: SP6T shorting type.
P: plug. F: 2.5 amp. fuse. LP_1, LP_2: 6.3 v. pilot lamps. R_L: Struthers Dunn 3AXX100 overload relay. SR: Federal 179115 selenium rectifier. SPK: 3 in. Utah PM: 3 Ω v.c. B_1, B_2: 22.5 v. hearing aid. B_3: 1.5 v. flashlight. L_1: 30 h. L_2: 30 mh.

FIG. 2. An instrument for leak detection and pressure measurement in high vacuum systems.

It was found convenient to use an aural indicator for leak detection to avoid continual observation of the meter. This was accomplished by means of a voltage-sensitive relaxation oscillator of the type described by Wouk (8). It consists of the tubes V_7, V_8, V_9, and V_{13}, a loudspeaker, and associated parts. The voltage developed across R_8 and R_9 is partially nullified by B_1 while R_{10} provides sensitivity adjustments. The frequency of oscillation is adjusted by varying the bias on V_7 by means of B_2 and R_{12} and the volume by R_{32}. Leaks can also be detected when the gauges are being used for pressure measurement by applying the voltage developed across the resistors R_{41} to R_{44} to the oscillator by means of the switch S_5. However, the saturated diode leak detector was found more sensitive.

HIGH VACUUM PROCEDURE

When the high vacuum equipment is built leaks frequently occur, and even with considerable ingenuity and experience one may expend a great deal of time and effort in tracing them. The following points should be borne in mind when equipment of this type is put into operation.

As pointed out above, the high vacuum system was for a mass spectroscope. It was constructed of brass and the gaskets consisted either of teflon as described by Nier (6) or of aluminum wire (1). It is advisable to place the vacuum thermocouples between the mechanical and diffusion pumps. If, when the mechanical pump is turned on, it is found that the pressure cannot be reduced to the 10^{-1} required for the operation of the diffusion pumps, the leak can be detected by a drop in the electromotive force of the thermocouple when methyl alcohol or other suitable liquid is sprayed onto the outside of the metal system. With the thermocouple gauge on the high vacuum system, the sensitivity to this test becomes negligible. Differential Pirani gauges (4) are more sensitive than thermocouples but the latter are quite satisfactory for detecting leaks at pressures down to those required for the operation of the diffusion pump. Serious leaks at pressures above 0.5 mm., which cannot be detected by thermocouples, can be traced by a hissing sound when the pumps are turned off or by immersion of the apparatus in water and application of an internal air pressure so that bubbles appear at the leaks.

It is often found that when the mechanical pumps are turned on, low pressures are not obtained even though there are no leaks. If the pump is left on for a few hours and the pressure falls steadily, degassing is probably responsible, but if the pressure remains constant, the cause is either a leak or water in the pump. The latter may be detected by pumping for about 15 min. with a large air leak so that a pressure of about 200 mm. of mercury is maintained. When the air leak is closed, the pressure falls below the previous minimum if the pump oil needs changing.

The ionization gauges are placed in the system nearest to the most likely sources of leaks (i.e., electrode connections or gaskets) by means of as short and as large a lead as possible. When the diffusion pumps are first turned on, the thermocouple gauges usually show an increase in pressure caused by

degassing of the pump oil, but after about half an hour the pressure begins to decrease. When it reaches about 7×10^{-2} in the foreline, the ionization gauges may be turned on and used either for pressure measurement or for leak detection as described above. Major leaks must be located first, because the filament is poisoned by air which enters through them, thus masking the effect of oxygen penetrating the smaller leaks.

A convenient method of sealing leaks in an all-metal system was by means of Araldite 985-E (sold by Ciba) prepared as a dipping varnish. After a leak has been brushed over with the system at atmospheric pressure, the surface is baked by means of a blue Bunsen flame. The varnish will stand a moderate amount of reheating.

ACKNOWLEDGMENTS

REFERENCES

1. BACHMAN, C. H.   Techniques in experimental electronics. John Wiley & Sons, Inc., New York. 1948. p. 58.
2. Central Scientific Company.   Thermocouple Gauge Control Unit, Cat. No. 94181. 1950.
3. DUSHMAN, S.   Scientific foundations of vacuum techniques. John Wiley & Sons, Inc., New York. 1949.
4. JACOBS, R. B. and ZUHR, H. F.   New developments in vacuum engineering reported in engineering developments in the gaseous diffusion process.   *Edited by* Benedict, M. and Williams, C. McGraw-Hill Book Company, Inc., New York. 1949. p. 48.
5. LEGER, E. and OUELLET, C.   J. Chem. Phys. 21: 1310. 1953.
6. NIER, A. O.   Rev. Sci. Instr. 18: 398. 1947.
7. RICHARDS, P. I. and TUTHILL, A. W.   Rev. Sci. Instr. 22: 841. 1951.
8. WOUK, V.   Electronics, 19: 138. 1946.

FREQUENCY MULTIPLICATION BY REGENERATIVE MODULATION[1]

By D. Makow

ABSTRACT

Circuits are described by which generation of multiples of a given frequency can be achieved by means of regenerative modulation. A separation between the even and the odd multiples on two different output terminals is possible. Maximum amplitudes can be obtained in a desired multiple range. The ability of such regenerative modulation circuits to produce the various frequency components is to a large extent independent of the variations of the input, filament, and plate voltages. In addition, phase shift in the feedback loop, which is troublesome in many regenerative circuits, is of no consequence.

INTRODUCTION

The most widely used method for generation of multiple frequencies from a given frequency introduces distortion to the original wave form. The distorted wave may be made to contain the desired multiples, but if the order of the multiple is high, say greater than five, the amplitude is almost certain to be too small for ready use. Furthermore, since the amplitude of the multiple depends on the kind and amount of distortion introduced, its amplitude may vary considerably with the changes in input and power supply voltages.

A basically different approach for generation of multiple frequencies uses mixing processes in a regenerative modulation circuit. Such regenerative modulation circuits have been treated in the literature (1, 2), but so far as the author is aware they have never been used to date for generation of multiple frequencies. In regenerative modulation circuits described in the prior art, the feedback voltage was essentially of one frequency. It has been found that oscillation can also be maintained in a suitably designed circuit, when the feedback voltage wave form contains several frequencies. Only those frequencies can be maintained which are rationally related to the frequency of the input. Circuits of this type can be used as multiple or fractional frequency generators.

An experimental circuit using regenerative modulation for generation of multiple frequencies has been developed and is described below (see Fig. 3). One of its characteristics is the ability to generate the odd and even multiple frequencies at two different output terminals, a property which permits the separation of the various frequency components with less filtering than would otherwise be required. The multiple frequencies have their maximum amplitude in certain frequency regions. This fact may be of value in cases where one is interested only in a group of frequencies in a desired frequency range, for example, in the case of U.H.F. multichannel radio communication, or in certain frequency standard work.

In general, it has been found that this circuit retains the performance characteristics of regenerative modulation circuits. The generation of the multiple frequency components is satisfactory in the presence of variations in plate, filament, or input voltage, as well as when aging components introduce phase-shift in the loop. This circuit is applicable wherever amplification and mixing are possible.

THEORY

(a) Conditions of Operation

A block diagram of five interconnected circuit elements is shown in Fig. 1. It consists of two mixers MI and MII, and three filter–amplifier combinations


$(f_p+f)-(f_1-f),\ (f_p+f)-(f_2-f),$
$(f_p+f)-(f_3-f),\ \ldots\ (f_p+f)-(f_m-f),\ ..$
$(f_p+f)-(f_p-f),$
$(f_p+f)-(f_1+f),\ (f_p+f)-(f_2+f),$
$(f_p+f)-(f_3+f),\ \ldots\ (f_p+f)-(f_m+f),\ \ldots$
$(f_p+f)-(f_{(p-1)}+f)$

$f_1, f_2, f_3, \ldots f_m \ldots f_p$

$f_1-f,\ f_2-f,\ f_3-f,\ \ldots$
$f_m-f,\ \ldots\ f_p-f,$
$f_1+f,\ f_2+f,\ f_3+f,.$
$f_m+f,\ \ldots\ f_{(p-1)}+f$

f_p+f
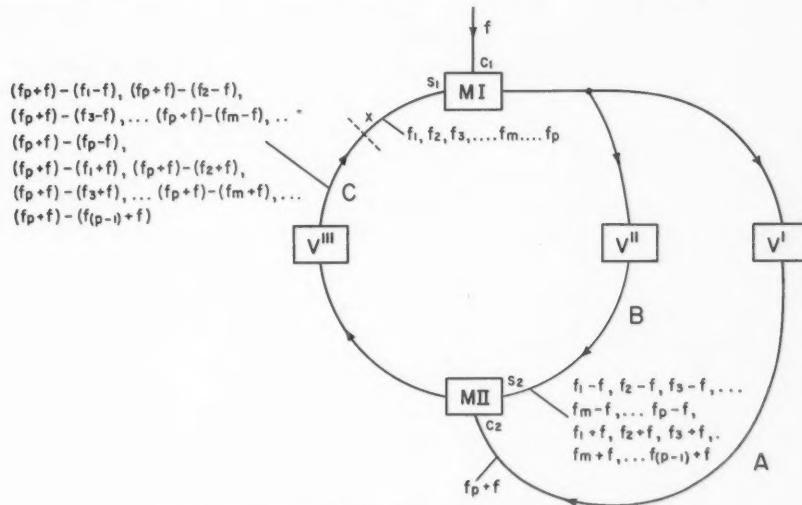
Fig. 1. Block diagram illustrating the principle of the circuit.

V', V'', and V'''. Assume that each mixer adds or subtracts the signal frequencies at input s to or from the carrier frequency at input c. In the case of mixer MI the signal frequencies at s_1 are:

[1] $$f_1 < f_2 < f_3 \ldots < f_m < \ldots < f_p$$

and the carrier frequency is $f < f_1$.

Assume that the filter in V'' is a low-pass filter designed to pass all frequencies smaller than f_p+f, and the filter in V' is a band-pass filter designed to pass the lowest sum frequency only, f_p+f. Then the signal frequencies at terminal s_2 of MII are $f_1-f, f_2-f, f_3-f, \ldots, f_m-f, \ldots, f_p-f, f_1+f, f_2+f, f_3+f, \ldots, f_m+f, \ldots, f_{(p-1)}+f$, and the carrier frequency at terminal c_2 is simply f_p+f.

Assume that the filter in V''' is a low-pass filter designed to pass all frequencies smaller than f_p+f, so that only the difference frequencies of the MII

inputs are passed; namely, $(f_p+f)-(f_1-f)$, $(f_p+f)-(f_2-f)$, $(f_p+f)-(f_3-f)$, $\ldots$, $(f_p+f)-(f_m-f)$, $\ldots$, $(f_p+f)-(f_p-f)$, and $(f_p+f)-(f_1+f)$, (f_p+f) $-(f_2+f)$, $(f_p+f)-(f_3+f)\ldots$, $(f_p+f)-(f_m+f)$, $\ldots$, $(f_p+f)-(f_{(p-1)}+f)$.

If the loop is to be closed at the point x and the system oscillate, this series of frequency components, passed by the filter in V''', must equal the series of signal frequencies assumed at s_1 in number of components present, in value of the components, and in the amplitude and phase of each component; and the frequencies in the series must be rationally related to maintain a periodic wave.

As a simple example consider the case where $p = 2$. Higher values of p will be discussed later. Then the input signals at s_1 will be f_1 and f_2, and the output frequencies at V''' will be:

$$(f_2+f)-(f_1-f),$$
$$(f_2+f)-(f_2-f),$$
and $\qquad (f_2+f)-(f_1+f).$

Since there is an extra component in the output series, two of the components must be equal. Since $f < f_1 < f_2$ the only possible equality is:

$$(f_2+f)-(f_1+f) = (f_2+f)-(f_2-f)$$

or,

[2] $\qquad\qquad f_2 = f_1+2f.$

Then, setting the remaining component of the output series equal to the second component of the signal series, it is found that:

[3] $\qquad\qquad f_1 = 2f.$

Combining [2] and [3]:

[4] $\qquad\qquad f_2 = 4f.$

In the general case it can be shown that the branches will contain the following multiples of the input frequency:

$$\text{Branch A}\quad (2p+1)f.$$
$$\text{Branch B}\quad f,\, 3f,\, 5f,\, \ldots,\, (2p-1)f.$$
$$\text{Branch C}\quad 2f,\, 4f,\, 6f,\, \ldots,\, 2pf.$$

The higher order frequency components found at the output of MI or MII will not deliver any new frequency components, because they will be either rejected by the low-pass filter in V'' or V''', or they will coincide with the useful frequencies, since the output frequencies of a balanced ring modulator are (3):

$$kf_c \pm f_s$$

where f_c is the carrier frequency, f_s is the signal frequency, and k an odd integer. Also, in this case f_s is rationally related to f_c. For modulator MI, f_m is an even multiple of f, and converts into an odd multiple for any value of k. Likewise, for modulator MII, $f_m \pm f$ and f_p+f are all odd multiples of f and hence all its output frequencies will be even multiples of f.

Thus, only frequencies rationally related to the input frequency are possible in this system. Branch B contains the odd multiples of f and branch C the even ones. The number of multiples p in branch C is determined by the value of the cutoff frequencies of the filter in V''' and V'''' and the center frequency of the filter in V'.

Next consider the amplitude and phase relationship in the loop for the case $p = 2$. Let the amplifier–filter unit V' introduce a gain μ_n' and phase shift a_n' for the frequency f_n. Likewise, let V'' and V'''' introduce gains μ_n'' and μ_n''' and the phase shifts a_n'' and a_n''' respectively for the frequency f_n.

Consider the loop to be cut at x (see Fig. 1). Then for the steady state condition voltages on one side of the intersection must equal voltages of the same frequencies on the other side.

Let the voltage $A \cos(2\pi ft)$, large enough to cause switching, be applied to MI at the input c_1, and let voltages $A_2 \cos(4\pi ft+\phi_2)$ and $A_4 \cos(8\pi ft+\phi_4)$ be applied at the input s_1. Now the low-pass filter in V'' and V'''' reject frequencies $5f$ and higher, so that μ_5'' and μ_5''' are equal to zero. Likewise, the band-pass filter in V' passes $5f$ only, so that μ_1', μ_2', μ_3', and μ_4' are all equal to zero. The contribution to the frequency components at the output of MI and MII due to higher modulation products will be neglected.

The modulation components of MI, which are passed by V'' and are applied to the s_2 input of MII, will be:

$$A_2 G \mu_3'' \cos(6\pi ft+\phi_2+a_3'') + A_4 G \mu_3'' \cos(6\pi ft+\phi_4+a_3'')$$
$$+ A_2 G \mu_1'' \cos(2\pi ft+\phi_2+a_1'').$$

G is the conversion gain (less than unity) of a balanced ring modulator, and is assumed to be the same for MI and MII.

Likewise the modulation component found at the c_2 input of MII will be:

[5] $$A_4 G \mu_5' \cos(10\pi ft+\phi_4+a_5').$$

The amplifier–filter unit in V'''' will pass only the difference components of MII, namely:

$$A_2 G^2 \mu_3'' \mu_2''' \cos(4\pi ft+\phi_4-\phi_2+a_5'-a_3''+a_2''')$$
$$+ A_4 G^2 \mu_3'' \mu_2''' \cos(4\pi ft+a_5'-a_3''+a_2''')$$
$$+ A_2 G^2 \mu_1'' \mu_4''' \cos(8\pi ft+\phi_4-\phi_2+a_5'-a_1''+a_4''').$$

Then, equating at x for the voltage of frequency $2f$:

$$A_2 \cos(4\pi ft+\phi_2) = A_2 G^2 \mu_3'' \mu_2''' \cos(4\pi ft+\phi_4-\phi_2+a_5'-a_3''+a_2''')$$
$$+ A_4 G^2 \mu_3'' \mu_2''' \cos(4\pi ft+a_5'+a_3''+a_2''')$$

$$= A_2 G^2 \mu_3''\mu_2''' \sqrt{1+\left(\frac{A_4}{A_2}\right)^2+\frac{2A_4}{A_2}\cos(\phi_2-\phi_4)}$$

$$\times \cos\left\{4\pi ft+\phi_4-\phi_2+a_5'-a_3''+a_2'''+\tan^{-1}\left[\frac{(A_4/A_2)\sin(\phi_2-\phi_4)}{1+(A_4/A_2)\cos(\phi_2-\phi_4)}\right]\right\}.$$

The amplitude condition is obtained by equating the amplitudes:

[6a]
$$1 = G^2 \mu_3'' \mu_2''' \sqrt{1 + \left(\frac{A_4}{A_2}\right)^2 + \frac{2A_4}{A_2} \cos(\phi_2 - \phi_4)}.$$

Likewise, the phase condition is obtained by equating the phases:

[6b]
$$0 = \phi_4 - 2\phi_2 + a_5' - a_3'' + a_2''' + \tan^{-1}\left\{\frac{(A_4/A_2)\sin(\phi_2 - \phi_4)}{1 + (A_4/A_2)\cos(\phi_2 - \phi_4)}\right\}.$$

Also, for the voltage of frequency $4f$ the amplitude and phase conditions are:

[7a]
$$A_4/A_2 = G^2 \mu_1'' \mu_4''',$$

[7b]
$$0 = -\phi_2 + a_5' - a_1'' + a_4'''.$$

Equations [6a] and [6b] can be written as

[8]
$$1 = D\sqrt{1 + K^2 + 2K \cos C},$$

[9]
$$0 = -B - C + \tan^{-1}\left[\frac{K \sin C}{1 + K \cos C}\right]$$

where,

$$B = \phi_2 - a_5' + a_3'' - a_2''',$$
$$C = \phi_2 - \phi_4,$$
$$D = G^2 \mu_3'' \mu_2''',$$
$$K = A_4/A_2.$$

A_4/A_2 and ϕ_4 can be found by solving equations [8] and [9] for K and C and observing equation [7b].

The significant values for A_4/A_2 and ϕ_4 are:

[10] A_4/A_2
$$= \frac{\cos(a_3'' - a_1'' + a_4''' - a_2''') \overset{(+)}{\underset{-}{}} \sqrt{G^4 \mu_3''^2 \mu_2'''^2 - \sin^2(a_3'' - a_1'' + a_4''' - a_2''')}}{G^2 \mu_3'' \mu_2'''},$$

[11] $\phi_4 = a_5' - a_1'' + a_4'''\overset{(-)}{\underset{+}{}} \sin^{-1}\left\{\dfrac{\sin(a_3'' - a_1'' + a_4''' - a_2''')}{G^2 \mu_3'' \mu_2'''}\right\}.$

In the usual case filters V'' and V'''' will be flat over their respective pass-bands, so that $\mu_1'' = \mu_3'' = \mu''$ and $\mu_2''' = \mu_4''' = \mu'''$. Then A_4/A_2 can be found by solving equations [7a] and [10].

[12] $A_4/A_2 = G^2 \mu_1'' \mu_4''' = G^2 \mu_3'' \mu_2''' = G^2 \mu'' \mu'''$

$$= [\tfrac{1}{2}\{2\cos(a_3'' - a_1'' + a_4''' - a_2''') + 1\}$$
$$\overset{(+)}{\underset{-}{}}\sqrt{(\tfrac{1}{2})^2\{2\cos(a_3'' - a_1'' + a_4''' - a_2'') + 1\}^2 - 1}]^{\frac{1}{2}}.$$

Inspection of equation [12] shows that real values for A_4/A_2 are possible for:

$$-60° < (a_3'' - a_1'' + a_4''' - a_2''') < +60°.$$

The phase shifts a_1'' and a_3'' are phase shifts through the same amplifier–filter unit at different frequencies, and in practice the difference between them

will be small. Likewise, the difference between a_2''' and a_4''' is small. Hence $\cos(a_3'' - a_1'' + a_4''' - a_2''')$ is nearly equal to unity, $\sin(a_3'' - a_1'' + a_4''' - a_2''')$ is nearly equal to the angle in radians, and the equations [12] and [11] reduce to [13] and [14]:

[13] $\quad A_4/A_2 = G^2 \mu'' \mu''' = \sqrt{\tfrac{1}{2}(3 - \sqrt{5})} = \tfrac{1}{2}(\sqrt{5} - 1) \cong 0.618,$

[14] $\quad \phi_4 = a_5' - a_1'' + a_4''' \overset{(-)}{\underset{+}{}} 2(a_3'' - a_1'' + a_4''' - a_2''')/(\sqrt{5} - 1),$

[15] $\qquad\qquad\qquad\qquad \phi_2 = a_5' - a_1'' + a_4'''.$

Equations [13] and [14] together with condition [15] (see equation [7b]) represent the amplitude and phase relationship in the loop for the case $p = 2$.

The conversion gain of a balanced ring modulator increases with increasing carrier voltage to a constant value approximately equal to $2/\pi k$ (see Ref. 3). At the same time the amplification factors μ'' and μ'''' eventually decrease with increasing grid voltage. Then equation [13] is satisfied when the amplitudes of oscillation for frequencies $3f$ and $2f$, or f and $4f$ respectively, are great enough to balance the losses in the modulator MII with the gain in the amplifiers. Since the input voltage is the carrier voltage of MI, there will be a threshold value of the input voltage above which operation of the circuit is possible. The carrier voltage of a ring modulator should be N-times greater (3 to 10 times for satisfactory operation) than the signal voltage; hence the required amplification μ_5' in the amplifier–filter unit V' is approximately given by:

[16] $\qquad\qquad\qquad\qquad \mu_5' \geqslant N\mu''.$

It is observed that the phase conditions [14] and [15] are always met since ϕ_2 and ϕ_4 are simply functions of the phase shifts in the amplifier–filter units. Thus no phase adjustments are necessary, either by automatic shift in frequency or by deliberate design.

(b) *Relationship between Amplitude of Oscillation and Input Frequency*

Next, the relationship between the amplitudes of the multiples and the input frequency will be considered.

The relative phase ϕ_5 of $5f$ at c_2 in respect to f at c_1 is

[17] $\quad \phi_5 = 2a_5' - [a_1'' - a_4''' \overset{(+)}{\underset{-}{}} 2(a_3'' - a_1'' + a_4''' - a_2''')/(\sqrt{5} - 1)] = 2a_5' - \lambda$

(see modulation component [5] and equation [14]) and the voltage amplitude of $5f$ is determined by the response characteristic of V' (see Fig. 2). As the input frequency increases a_5' will decrease, and to the higher frequency side the voltage amplitude of $5f$ will decrease until the conversion gain G of MII is too small to satisfy the gain condition [13] where the operation of the circuit stops. As the input frequency decreases, a_5' increases to the point where ϕ_5 goes through zero and becomes positive. Then the modulator MII introduces a phase-shift of $180°$ due to the reversal of the carrier voltage,
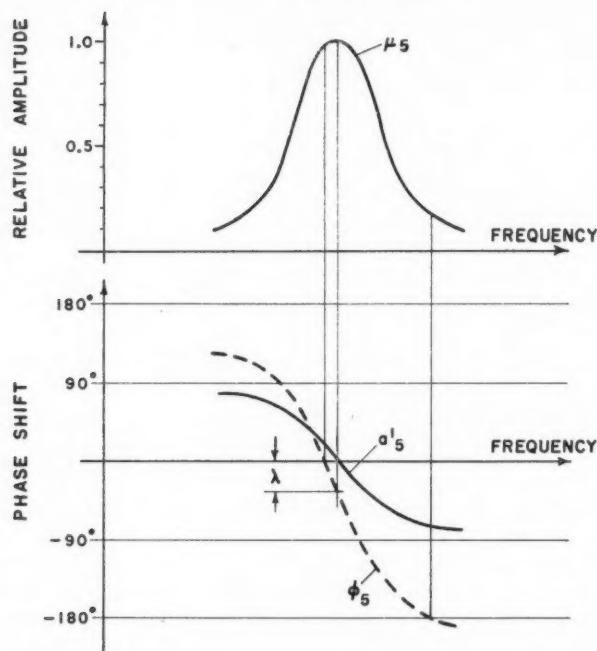
FIG. 2. Amplitude and phase relationship of the amplifier–filter unit V'.

and it can be seen from equation [12] that no real input is then possible. Likewise no real output is possible when ϕ_5 goes through $-180°$.

When λ is zero (see equation [17]) the point where ϕ_5 is equal to zero coincides with maximum voltage amplitude of $5f$, where the operation of the circuit stops. For finite values of λ, stopping of operation because of reversal of the carrier voltage would take place before or after the frequency where the amplitude of $5f$ is a maximum.

The same argument can be applied to the case where the input frequency is fixed, but where the center frequency of the filter in V' drifts.

Circuits for higher values of p could be analyzed in a similar manner but the number of unknowns is greater and the solutions are involved. Hence these cases were investigated experimentally.

EXPERIMENTAL WORK

(a) *Experimental Check of the Theory*

Experiments were carried out to verify the results of the theory, for the example $p = 2$, or $n = 5$, where n is the ratio of the carrier frequency of MII to the input frequency, and is equal to $2p+1$.

Fig. 3 shows the details of the circuit. The amplifier–filter units in V' and V'' are made up respectively of a 6AG7 pentode tuned stage and a 6SF5
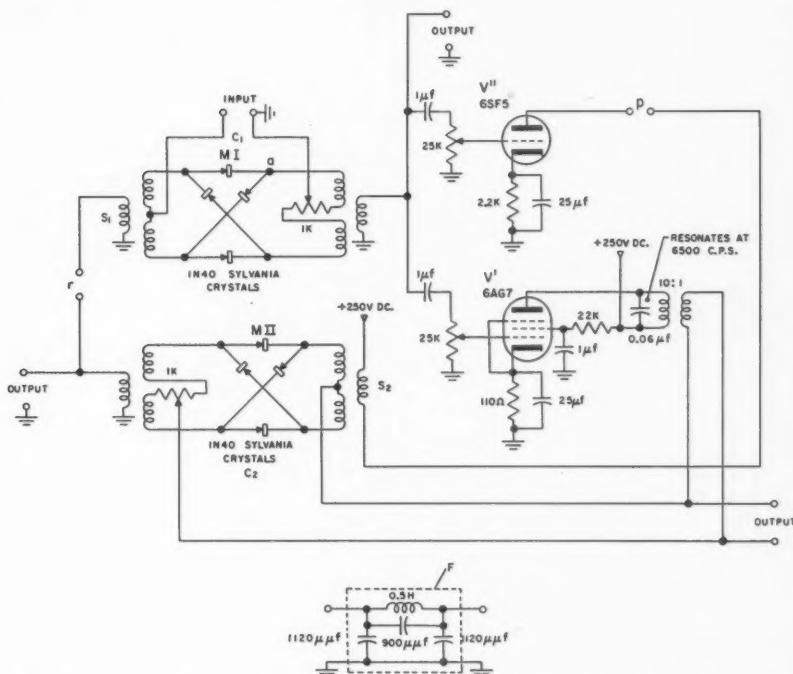
FIG. 3.   Circuit diagram of a frequency multiplier utilizing regenerative modulation.

triode with the filter F inserted at the position p. V''' is made up of the filter F only, inserted at the position r. No amplifier is necessary since the required loop gain can be supplied by the 6SF5 stage. The tuned circuit in V' employs a Ferroxcube pot core and has a Q of 35 at the frequency 6500 cycles per second.

It was found that the circuit is self-starting when there is sufficient gain in the loop, or when the input voltage is large. As the loop gain or the input voltage is reduced, there is a range where starting of operation could be accomplished by shorting the point "a" of MI to ground (see Fig. 3) thus momentarily introducing useful frequency components into the loop. A slight unbalance of MI also improves the self-starting ability of the circuit. As the gain in the loop or the input voltage is further reduced, starting of the circuit is not possible.

It was found that the circuit could be started at about 0.25 v. input when the gain is adjusted for minimum. As the input voltage increased from its minimum starting value, the amplitude of the multiples was found to increase to about double the original value and then remained constant for input voltages between 3 and 30.
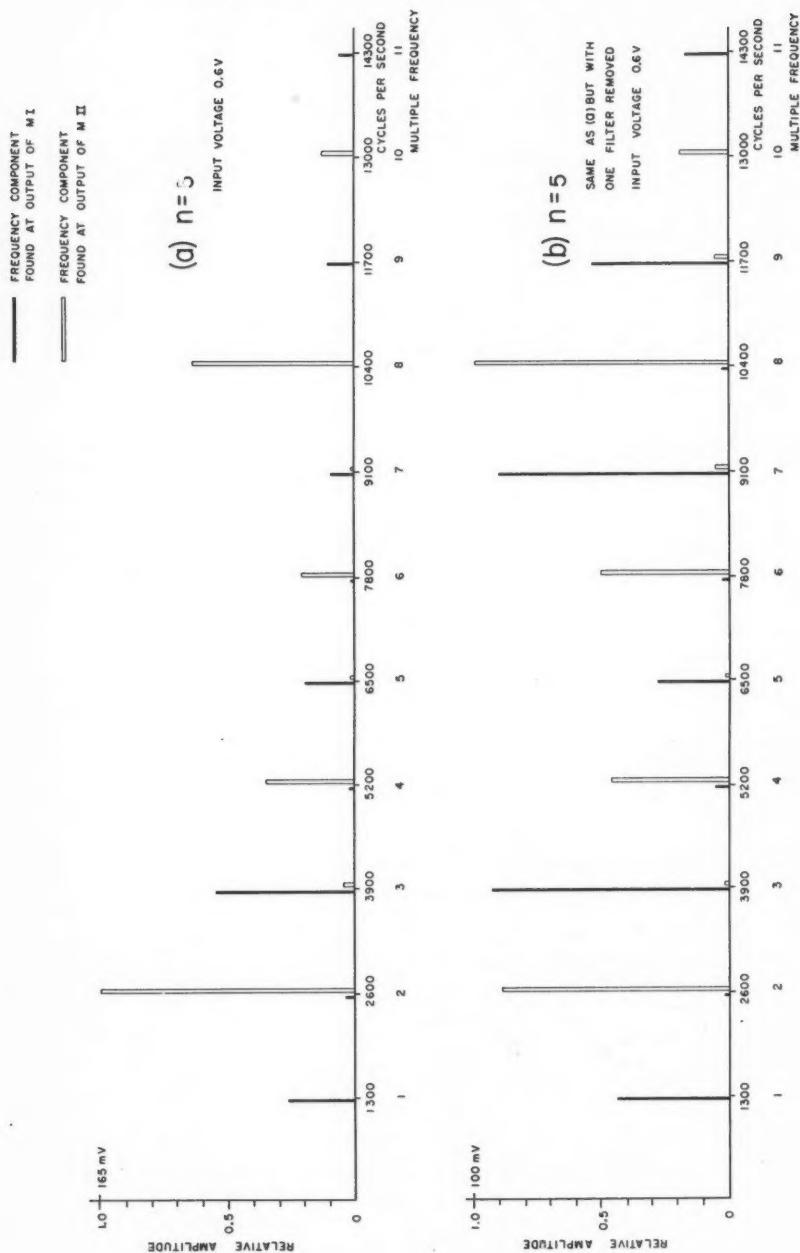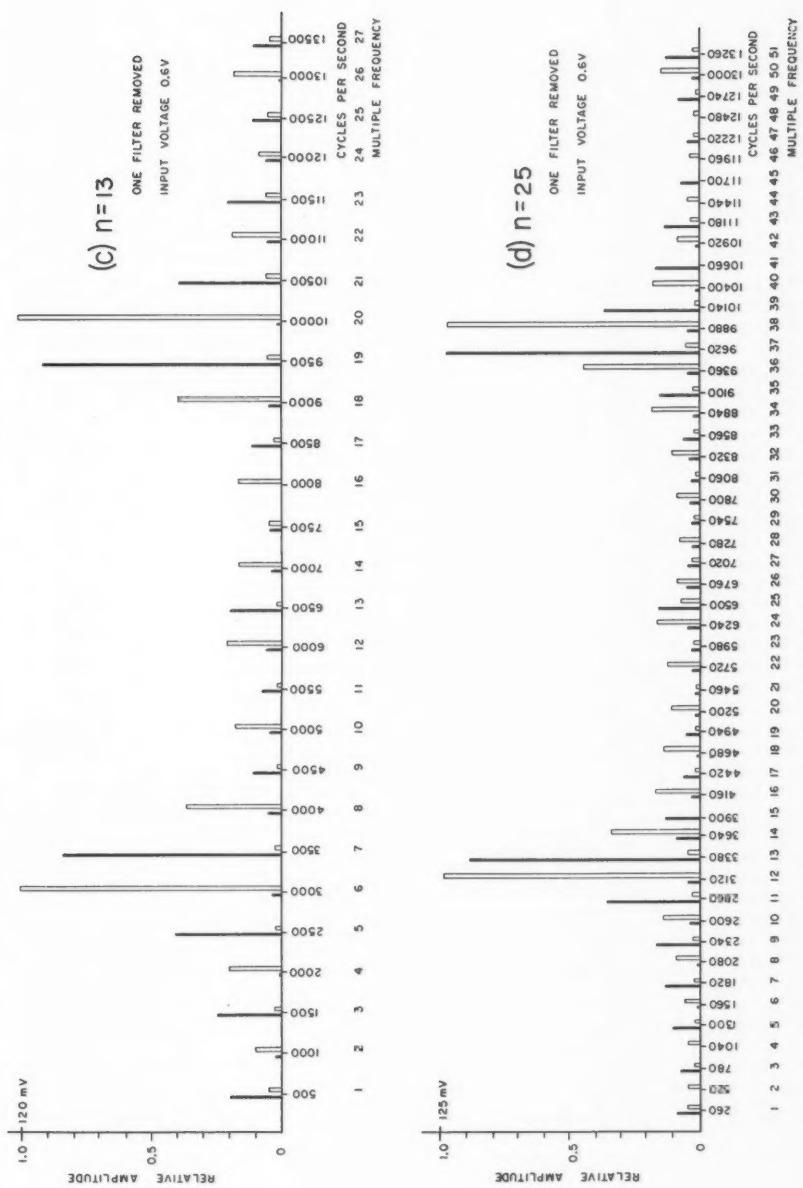
Fig. 4. Frequency spectra of the output voltages of the modulators MI and MII, measured with a wave analyzer.

The circuit operates in the range 50 v. to 300 v. plate voltage for 6.3 v. on the filament, and from 3 v. to 8.5 v. filament voltage for 250 v. on the plate.

The multiples of 1300 cycles per second found at the output of MI and MII were measured with a wave analyzer and are shown in graph (a) of Fig. 4. It can be seen that equation [13] is approximately fulfilled, and good discrimination between the odd and even multiples is realized.

The relationship between the amplitude of the multiples and the input frequency is shown in Fig. 5. For the multiple $5f$, this relationship has the same shape as the resonance curve of the tuned stage in V', but only one fifth of the width. The amplitude of f, $2f$, $3f$, and $4f$ is less influenced by the change of the input frequency and could be made almost independent of it if the carrier voltage of MII were large enough. A region of operation was obtained as predicted in the discussion and bounded by frequencies of 1290 and 1340 cycles per second. When the polarity of the input terminals of c_2 at MII was reversed, the region of operation jumped over to the other side of the maximum, as shown by the dashed lines.

(b) Operation with Only One Low-Pass Filter

It can be shown that operation with only one low-pass filter is possible, and under certain conditions, desirable.

First, consider the filter F placed at the position r (in Fig. 3) and the terminal p shorted. The highest possible multiple of f at s_1 is then $4f$, and the output of MI will not contain any multiples higher than $5f$. (Higher modulation products are relatively small and therefore neglected.) At the s_2 input of MII the frequencies f, $3f$, and $5f$ are present. f and $3f$ are useful, and $5f$ can be tolerated since it does not contribute to any multiples within the acceptance band of F. Thus in theory it should be possible to realize the same multiples with one low-pass filter as are realized with two.

Consider the second case, where F is inserted at the position p in Fig. 3 and the terminals r shorted. Then the s_2 input of MII contains the frequencies f and $3f$, and the s_1 input of MI contains $2f$, $4f$, $6f$, and $8f$. The output of MI contains f and $3f$; $5f$, $7f$, and $9f$ are rejected by the filter F. Therefore removal of the filter F from the position r does not affect the distribution of the multiples in the circuit. The multiple $5f$ may, however, have a larger voltage amplitude, since it receives energy contributions not only from $4f$ but also from $6f$.

Circuits of the second type have greater practical value than those of the first type, since higher multiples can be produced than by the general circuit. Moreover, not only the multiples of $2f$ and $3f$ will have maximum amplitudes, but also the multiples $7f$ and $8f$, as they are derived from $3f$. Measured values ·of the amplitudes of the multiples for $n = 5$ for this case are shown in graph (b) of Fig. 4.

(c) Experimental Investigation of Higher Values of n

It was decided to investigate the production of higher ratios using a circuit of the second type. The tuned circuit of the V' stage and the filter F were not
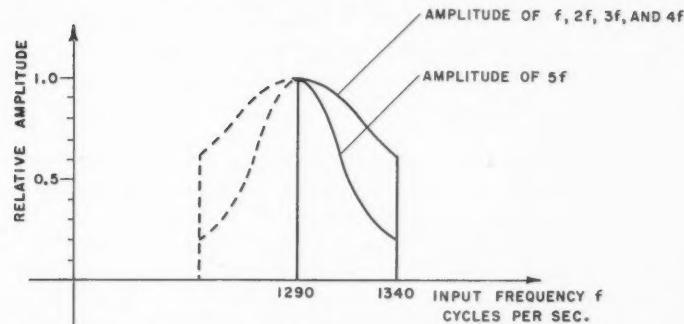
FIG. 5. Relationship between the amplitude of the frequency components generated in the frequency multiplier circuit and the input frequency, measured with a wave analyzer.

changed, but the frequency of the input voltage was decreased. Graph (c) of Fig. 4 shows the measured values of the amplitudes of the multiples for $n = 13$. Maximum values were found for $\frac{1}{2}(n \pm 1)f$ or $6f$ and $7f$, and for $[n + \frac{1}{2}(n \pm 1)]f$ or $19f$ and $20f$.

The amplitude distribution of the multiples for $n = 13$ can be explained as follows: Graph (a) of Fig. 6 shows how the energy contained in the individual multiples is transferred from one multiple to another. The dots indicate
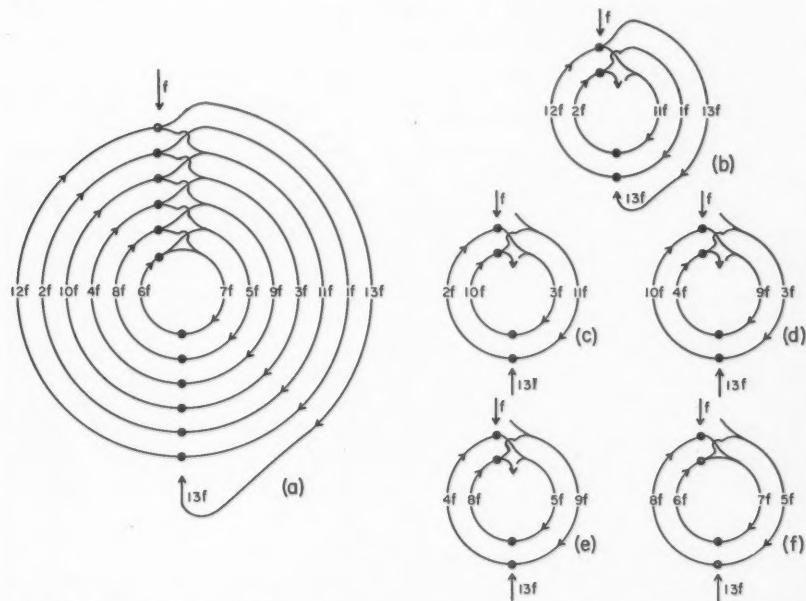

FIG. 6. Graphical representation of the closed loop system, formed by the flow of energy contained in the various frequency components generated in the frequency multiplier circuit.

conversion with f or $13f$ respectively. This multiloop system can be split into a series of simpler loops. Graph (b) of Fig. 6 shows how f, $11f$, $2f$, $12f$, and $13f$ can form a self-sustained loop. Suppose that all their amplitudes have the value A. Then the loop shown in graph (c) of Fig. 6 can be maintained also since $13f$ is present. It can be seen that $11f$, which was already present in the loop in graph (b) of Fig. 6, receives an additional energy contribution from $10f$, thus increasing its amplitude. Then also the amplitude level of the remaining multiples is affected so that $3f$, $11f$, $2f$, and $10f$ may reach the value $2A$ if the contributions from $10f$ and $12f$ are in phase. Likewise, in the loop shown in graph (d) of Fig. 6 the amplitudes of $9f$, $3f$, $4f$, and $10f$ may reach the value of $4A$. Similar action takes place in the loop in the graphs (e) and (f) of Fig. 6, and as a result the multiples $6f$ and $7f$ of the inner loop reach maximum amplitudes. Furthermore, the amplitude distribution for the multiples $13f$ to $25f$ (see graph (c) in Fig. 4) is a mirror image of the distribution for the multiples f to $13f$, because the former are either sum components of the MII inputs or modulation products of these sum components with f.

A similar amplitude distribution of the multiples was measured for the case $n = 25$ (see graph (d) of Fig. 4).

If only a single multiple of the input frequency is required, it is probably best to design the system to obtain this multiple at the output of V', since the amplitude is relatively high and no other multiples are present.

The relation between the amplitudes of the multiples and the input frequency was found to be similar to the case $n = 5$ for both $n = 13$ and $n = 25$, but the range of the input frequency for which operation of the circuit is possible is reduced. Likewise the relation between the amplitude of the multiples and the amplitude of the input voltage was found to be similar to the case $n = 5$, for both $n = 13$ and $n = 25$.

As n increased, the usable input and power supply voltage ranges were found to be reduced in the cases under consideration. Nevertheless, in the case $n = 25$, stable operation was observed when either variations of the input voltage from 0.3 to 2.7, or plate voltage from 180 to 300, or filament voltage from 4.5 to 8 were introduced; the two remaining voltages were set at the normal operating points in each case.

In general, the tuned circuit in V' should have a high enough selectivity to reject the adjacent multiples to a degree where the resulting low frequency beat does not influence the conversion gain of MII greatly. The degree of rejection will be of less importance for a larger carrier voltage at MII. It can be shown that in any case where the carrier voltage of MII is large enough to permit 33% amplitude modulation of nf by the multiples $(n \pm 2)f$, the required Q of the tuned circuit is:

$$Q = 1.5\,n$$

(see Terman: "Radio Engineering Handbook" p. 137).

In the case where the filter F is removed from position r in the circuit, this value of Q is reduced by the factor 0.5, since nf receives an additional contribution from $(n+1)f$.

The steepness of the filter F at the cutoff frequency should be such as to introduce little attenuation to the multiple $(n-2)f$ or $(n-1)f$ when inserted at position p or r respectively. This condition appears to be non-critical, since satisfactory operation for $n = 25$ was realized with a filter F designed originally for $n = 5$.

CONCLUSIONS

A circuit for generation of multiples of a given frequency using the method of regenerative modulation has been described. A theory has been developed for a circuit designed to produce four multiples of the input frequency and this theory has been confirmed experimentally. In addition, circuits to produce higher multiples were studied experimentally. Multiples up to the 40th were realized with good amplitudes, and it is believed that still larger multiplication ratios could be realized with this type of circuit. The generation of multiples was found to be unimpaired to a large degree by considerable variations of the power supply and input voltages, and phase-shift in the circuit.

ACKNOWLEDGMENTS

REFERENCES

1. MILLER, R. L.   Proc. I.R.E. 27: 446–457.   1939.
2. STANSEL, F. R.   Proc. I.R.E. 30: 157–162.   1942.
3. TUCKER, D. G.   J. Inst. Elec. Engrs. (London), III, 95: 161–172.   1948.

THE OXIDATION, DECOMPOSITION, IGNITION, AND DETONATION OF FUEL VAPORS AND GASES

XXIV. THE ADVERSE EFFECT ON THERMAL EFFICIENCY OF THE ENDOTHERMIC CRACKING REACTION REQUIRED FOR THE COMPRESSION IGNITION OF PARAFFIN HYDROCARBONS[1]

By R. O. King[2] and A. B. Allan[3]

ABSTRACT

The adverse effect on thermal efficiency of the decomposition (cracking) reaction required to produce the nuclei which enable a carburetor engine to run with ignition by compression is demonstrated by the experiments described in the text. For this purpose, values of indicated thermal efficiency determined when using normal varieties of pentane, hexane, and heptane with ignition by compression are compared with those determined when using benzene in comparable conditions of mixture strength and compression ratio. In these conditions benzene does not decompose during compression to the extent required to produce nuclei of ignition and mixtures with air require a spark for ignition, unless in contact with a surface at an igniting temperature. Values of indicated thermal efficiency determined when using the paraffins were from 7 to 8% lower than those obtained when using the benzene, mixture strength being 20% weak in both cases. The adverse effect increased with increase of mixture strength. It was approximately 10% for correct mixtures. Furthermore with nuclear ignition the paraffins could be used at weaker mixtures than was possible for benzene with spark ignition. The experiments indicate that the nuclear ignition of paraffin–air mixtures richer than 20% weak is a single stage effect due to carbon derived from cracking of the paraffin. The ignition of leaner mixtures occurs in two stages, the first being initiated by nuclei of a resinous nature. Residues of these nuclei mixed with carbon formed an adherent coating on surfaces not exposed directly to flame such as the lands between piston rings. The rings became firmly stuck in their grooves which had become filled with the residues. The experiments were carried out at diesel engine compression ratios and the results are believed to be of interest in respect of the fundamentals of combustion in that type of engine.

INTRODUCTION

The operation of a C.F.R.-F2 carburetor engine with ignition by compression when normal varieties of heptane, hexane, and pentane were used as fuels was described in Part XXI (4). The compression ratios required for ignition were comparable with those of diesel engines, as would be expected. They varied with mixture strength and the length of the carbon chain of the paraffin molecule. It was always possible to adjust compression ratio for a maximum power output at any particular mixture strength. The experimental results were consistent with the nuclear theory of ignition, as stated in Part IV (3), namely that the finely divided carbon required for the nuclear ignition of the end gas in a spark ignition carburetor engine is provided by the decomposition (cracking) of paraffinic fuel at the high temperatures and pressures attained.

On the other hand, it was shown by experiments described in Part XXII (5) that a hydrocarbon fuel such as benzene does not decompose at diesel engine compression ratios in a manner to provide nuclei of ignition. Decomposition if it occurred would, in the first stage, yield hydrogen and diphenyl which is a gas at the required temperatures. Thus in the experiments mentioned, a spark was always necessary for controllable ignition, and uncontrolled ignition tending to develop into preignition occurred when a spark plug core attained the requisite high temperature.

The experimental results of Parts XXI and XXII were in accordance with the well-known tendency of normal paraffins to decompose more readily to carbon and other final products than members of the aromatic series, in similar conditions of temperature and pressure. The decomposition reaction is endo-thermic and if it occurs during compression in an engine, thermal efficiency would be affected adversely by the heat absorbed. Thus it will be shown by the comparison made in this Part that (1) the thermal efficiencies obtained for the paraffins with compression ignition are lower than those obtained for benzene with spark ignition and (2) the paraffins with compression ignition can be used at mixtures leaner than those at which benzene can be ignited by spark ignition and that in these leaner mixtures nuclear ignition occurs in two stages, the first stage appearing to be due to nuclei containing resinous substances.

Arrangement of Text

Subsequent text is in numbered sections for convenience of reference. The normal paraffins are, when convenient, described as detonating fuels. The terms compression ratio, optimum compression ratio, mixture strength, indicated thermal efficiency, and indicated mean effective pressure are, when convenient, abbreviated to C.R., Opt.C.R., M.S., I.T.E., and I.M.E.P. respectively. Chemically correct mixtures of fuel and air are described as "correct" in the text but the abbreviation "C.C.M." is used on graphs. Values of compression ratio are abbreviated to a single number. Opt. C.R. is the value at which power output is a maximum at a particular mixture strength. Compression ignition is, when the context is fitting, described as nuclear ignition. It is to be understood that values for I.M.E.P. given in the text or on graphs are in pounds per square inch and that values given for engine speeds are revolutions per minute.

Heat Load

This term, although not commonly used, has been adopted as a convenient expression for the factors which determine the mean temperatures attained by surfaces in the combustion chamber, see discussion Part XXII (5, pp. 45–48). Primary factors are: the heat arising from compression of the fuel–air mixture and residual gases and the heat content of the entering mixture; plus the heat liberated by combustion of the fuel; minus the proportion converted into work, that absorbed by vaporization of fuel after admission, and that rejected to the exhaust. The heat load, expressed in B.t.u. per min. at parti-

cular values of C.R. and M.S., is then directly proportional to engine speed at constant volumetric efficiency. It will then be equal to the rate of heat conduction through the materials of the combustion chamber when engine temperatures have reached a steady state. The surface temperatures attained by materials in the combustion chamber will then depend on the temperature gradients in them. These in turn will depend on their thermal conductivities, the length and the nature of the heat path to the cooling medium, and its temperature. The surfaces of indirectly cooled parts of the combustion chamber are most liable to attain temperatures that will affect the combustion of the fuel. These are: the valves, the center of the piston crown, the ceramic core of the spark plug, and its electrodes. Any one of these, with an extremely heavy heat load, may attain the temperature required for some degree of flameless combustion of the fuel, but in normally aspirated water cooled engines, the surfaces liable to attain an igniting temperature in respect of the fuel–air charge are those of the exhaust valve, the ceramic core of the spark plug, and in some cases those of its electrodes—the exhaust valve because it is off its cooling seat during the exhaust stroke, the head and the lower part of its stem being then in the path of the exhaust gases, and the ceramic core of the spark plug because of its low thermal conductivity.

I. RATES OF BURNING OF PARAFFIN–AIR MIXTURES WITH NUCLEAR IGNITION AND OF BENZENE–AIR MIXTURES WITH SPARK IGNITION

Paraffin–Air Mixtures

Experiments with the paraffins, described in Part XXI (6), were carried out in engine conditions of a subnormal charge density, an air supply temperature of 50° F., a jacket coolant temperature of 100° F., and an engine speed of 400. That is, the heat load on the engine was relatively low and the corresponding low cycle temperature would be expected to be of favorable effect on indicated thermal efficiency. Ignition was by compression and maximum power output was obtained for values of the C.R. of 8.5, 9.6, and 10.0 for correct mixtures with air of heptane, hexane, and pentane, respectively. The characteristics of combustion are illustrated by the typical pressure–time diagrams of Fig. 1, taken when using heptane as the fuel. Short vertical lines have been added to the diagrams to mark the "blips" fed into the electronic circuit at 10° intervals of crank revolution by a notched timing wheel. The line at top dead center is marked t.d.c. The irregularity of spacing is due mainly to the inertia of rotating parts, including the armature of the direct connected generator, which was such that the speed of rotation of the blip timing wheel attached to the outboard end of the armature shaft was affected by cyclic changes of pressure on the piston. A relatively thick indicator diaphragm was used when taking diagram A, because of the high pressure developed. Therefore the pressure scale differs from that of diagram B. Both diagrams were taken with a "Sunbury" indicator and consequently the pressure scales are non-linear.

It will be seen by reference to the diagrams that nuclear ignition occurred in a single stage for mixtures correct and 20% weak. It occurred in two stages

for mixtures weaker than can be used for benzene with spark ignition. The characteristics of the two-stage effect will not be discussed at present. Diagram A, for a correct heptane–air mixture, shows that compression pressure ceased to rise appreciably at approximately 12° before t.d.c. and remained substan-
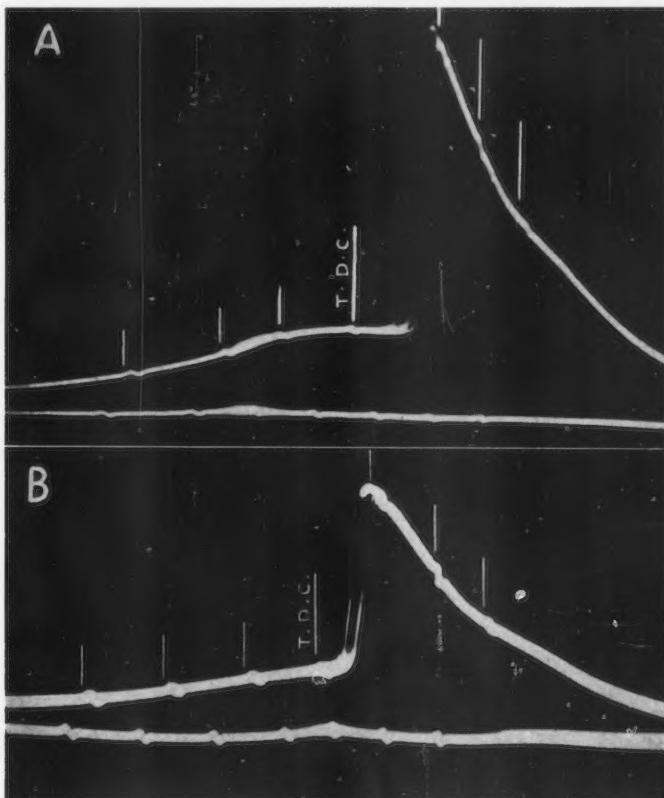

Fig. 1. Typical diagrams for the combustion of paraffins with nuclear ignition.
A. Correct mixture, C.R. 8.5.
B. 20% weak mixture, C.R. 9.1.
    Heptane.

tially constant until 7° after. The failure of pressure to rise during 19° of crank revolution is attributed to the absorption of heat by the decomposition reaction required to produce nuclei of ignition. It is the familiar "delay angle" which is a characteristic of the combustion of paraffinic fuels in diesel engines.

The combustion characteristics of the nuclear ignition of the 20% weak heptane–air mixture are shown by diagram B. This diagram, like diagram A, was taken when C.R. was adjusted for maximum power output and it will be

noted that, as for diagram A, this was obtained when combustion pressure attained a maximum value at approximately 10° after t.d.c. The Opt. C.R. was 9.1 and it appears from the compression line of the diagram that decomposition of the heptane at the gas temperatures and pressures attained accordingly began earlier than when the C.R. was lower, at the value of 8.5, as required to obtain maximum power output for a correct mixture, diagram A. A definite value cannot be assigned to the delay angle for the weaker mixture in the absence of a diagram for compression of air only. Both diagrams show that the pressure rise due to combustion started sharply at the end of the delay period, presumably on the attainment of the requisite concentration of nuclei in the part of the combustible mixture at maximum temperature. That would be the part adjacent to the exhaust valve, the spark plug having been replaced by a mild steel blank. The time interval between nuclear ignition and the attainment of maximum combustion pressure was 3° of crank revolution or 0.00125 sec. If the distance of flame travel is taken from the center of the exhaust valve to the farthest point on the combustion chamber wall, the velocity would be 150 ft./sec. In the circumstances and in the cool running conditions, the engine ran on a nearly exact constant volume cycle of relatively low temperature with maximum combustion pressure occurring at the piston position for maximum power output. Indicated thermal efficiency should therefore have approached the ideal value as nearly as possible in practice, *but for the loss during compression and prior to ignition of the heat absorbed by the decomposition reaction required to produce an igniting concentration of nuclei.* This loss would affect compression pressure adversely with the result that the engine would be running on a compression ratio lower than the measured value which is used when calculating thermal efficiency.

Benzene–Air Mixtures

The slow burning characteristic of benzene and its failure to decompose in the end gas of a spark ignition engine to provide the nuclei of ignition required for "detonation" are attributed to the stability of its molecule. A further consequence of slow burning is that in the experiments described in Part XXII (5), benzene was not a good fuel for the C.F.R. engine when operated in conditions of low heat load, in that when an attempt was made, by raising the compression ratio, to obtain maximum thermal efficiency for weak mixtures, the engine tended to run on a constant pressure instead of a constant volume cycle (5, pp. 27–28). An approach to a constant volume cycle was obtained for mixtures in the neighborhood of correct on increasing the heat load by raising the air supply from 50 to 140° F., the jacket coolant from 100 to 140° F., the speed from 400 to 900 r.p.m., and the charge density from 64% of normal to normal. It was estimated that these increases had resulted in raising the initial temperature of compression from 100 to 200° F. and the final temperature from 740 to 930° F. when the C.R. was 8.0 (5, p. 43). The characteristics of combustion obtained accordingly at the C.R. of 8.0 are illustrated by the typical indicator diagrams of Fig. 2. The time of passage of the spark is shown on the diagrams by the small downward blip fed into the electronic circuit. Optimum

spark timing was always used and it will be seen by reference to diagram A, that the spark occurred at 11° before t.d.c. and maximum pressure at 13° after. When a 26% weak mixture was used, diagram B, optimum spark timing was 21° in advance of t.d.c. and maximum combustion pressure occurred at 15° after.
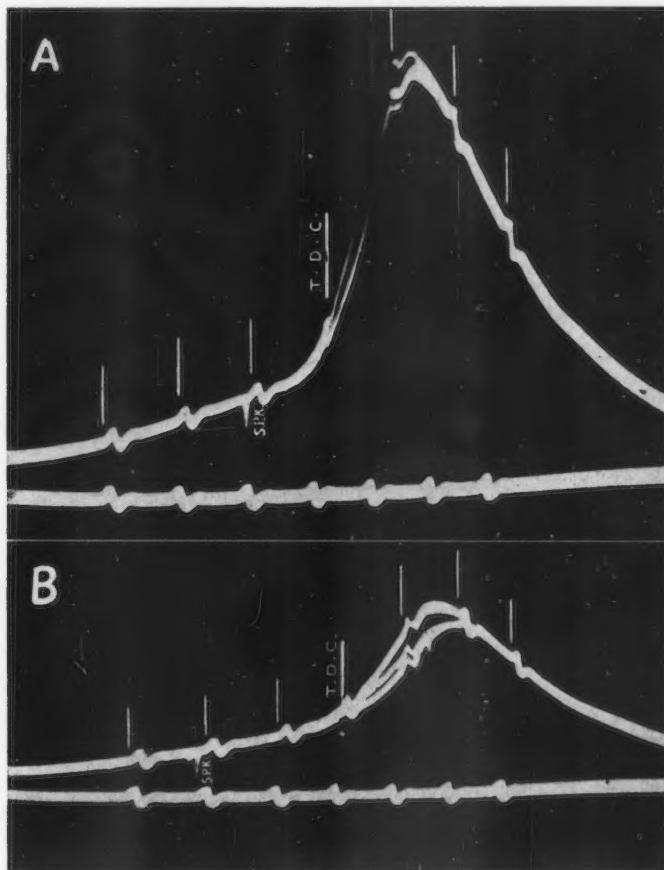

FIG. 2.   Typical diagrams for the combustion of benzene with spark ignition.
A. Correct mixture, C.R. 10.
B. 26% weak mixture, C.R. 8.

The long burning time required for the combustion of the benzene–air mixture even after increasing inflammability by raising the temperature of the charge at the time of spark ignition is in sharp contrast with the 3° of crank revolution required for combustion when nuclei of ignition had been provided by the preflame decomposition of a normal paraffin.

II. NUCLEAR IGNITION AND THE RELATION BETWEEN INDICATED THER-
MAL EFFICIENCY AND COMPRESSION RATIO; PENTANE, HEXANE, AND
HEPTANE

It was shown by experiments with the normal paraffins used in engine running conditions in which nuclear replaced spark ignition that the relation between Opt. C.R. and M.S. is represented by a W form of graph instead of the U form obtained when ignition is by spark at relatively low values of C.R., Part XXI (6). The W form of graph shown at A, Fig. 3, is for pentane–air mixtures and is similar in form to those obtained when using hexane and heptane. These will be given later as required. The corresponding relation between I.T.E. and
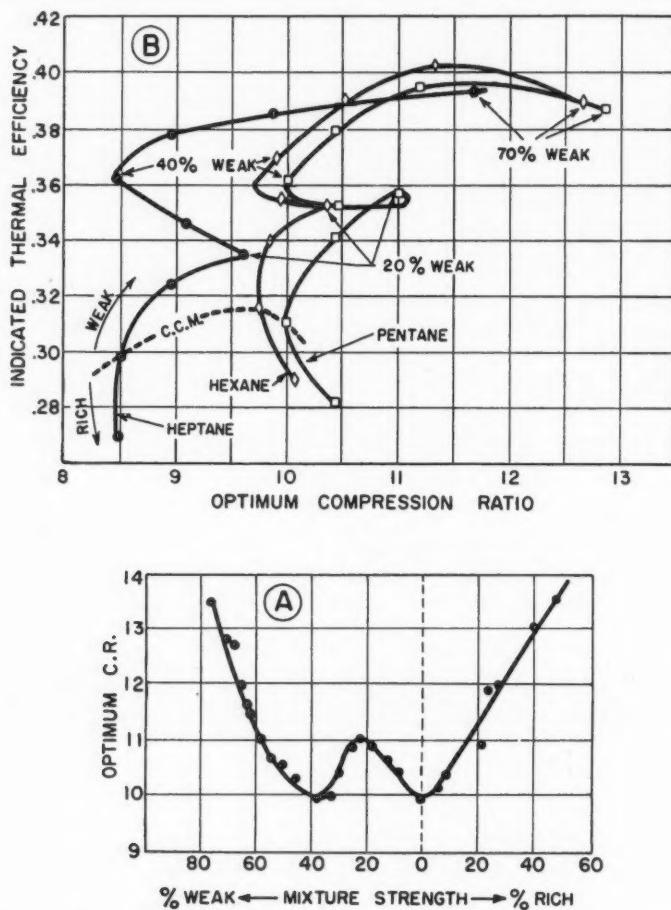
FIG. 3.   A. Typical relation between Opt. C.R. and M.S. shown by experiments with pentane.
B. Relation between I.T.E. and C.R. with diminishing M.S.; heptane, hexane, and pentane.

C.R. for mixtures with air of pentane, hexane, and heptane ranging from 10% rich to 70% weak, as determined by experiments described in Part XXI, are exhibited by the corresponding graphs, B, Fig. 3. They were not given earlier because comparable results for a non-detonating hydrocarbon with spark ignition were not then available. Experimental points are not shown on the graphs. They have been replaced by points indicating 10% changes of mixture strength. Correct mixtures are indicated by the broken line crossing the graphs.

Indicated thermal efficiency is shown by the graphs to have increased, as would be expected as Opt. C.R. was increased and mixture strength decreased from correct until it became 20% weak. An abrupt reversal of direction of the graphs then occurred and I.T.E. remained nearly constant over the mixture range 20 to 40% weak for both pentane and hexane. It will be noted however by reference to the A graph, that Opt. C.R. ratio diminished over this range of M.S. It appears therefore that the increase in I.T.E. normally due to a decrease of M.S. was just offset by the decrease in I.T.E. due to decrease of Opt. C.R. Nuclear ignition of heptane–air mixtures occurred at considerably lower compression ratios than were required for mixtures with air of pentane or hexane. The adverse effect on I.T.E. of decreasing Opt. C.R. over the mixture range 20 to 40% weak was, as shown by the graph, more than offset by the beneficial effect obtained on decreasing the M.S.

The graphs for I.T.E. show that another abrupt reversal of direction occurred for all three fuels when the mixtures became 40% weak. Then as mixture strength was further decreased and Opt. C.R. increased, I.T.E. increased slowly to a maximum value and then diminished. This characteristic is related to the occurrence of ignition and combustion in two stages, with the first beginning before t.d.c., Part XXI (6, Figs. 3 and 4).

The decomposition of heptane in correct mixtures with air, to provide nuclei of ignition at a C.R. of 8.5 whereas values of C.R. of 9.6 and 10 were required to obtain a similar effect in respect of hexane and pentane respectively affords a rational explanation for the use of heptane to represent zero on the C.F.R.–A.S.T.M. knock rating scale.

III. THERMAL EFFICIENCIES: BENZENE

Indicated Thermal Efficiencies at Values of C.R. from 4 to 13

The values of I.T.E. for benzene–air mixtures varying from 20% rich to the weakest on which the engine would run, and at values of C.R. increasing from 4 to 13, as determined by experiments described in Part XXII (5), are given by the graphs of Fig. 4. The operating conditions were those of the "higher" heat load. There are three features of the experimental results of especial present interest:

(1) The I.T.E. at any particular C.R. increased continuously, although at a decreasing rate as M.S. was reduced, as would be expected, until it had attained a maximum value when it diminished rapidly as misfiring began.

(2) The M.S. for which a maximum value of I.T.E. was obtained diminished with increase of C.R., as shown by the inclined broken line crossing the graphs of the figure. That is, misfiring occurred with progressively weaker mixtures as compression ratio was raised. Thus at a C.R. of 13, smooth running without misfiring continued until the mixture became 35% weak, but at a C.R. of 4, misfiring began with mixtures leaner than 25% weak.

The I.T.E. obtained for a mixture weaker than that required for maximum thermal efficiency is therefore not regarded as a true value.
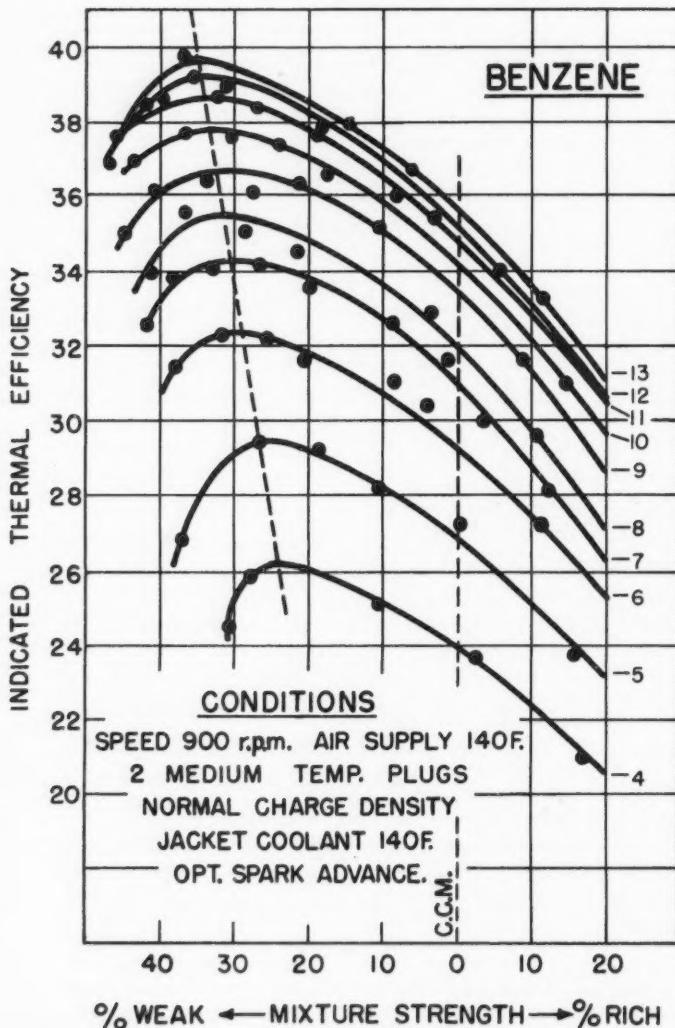
FIG. 4.   Relation between I.T.E. and M.S. at values of C.R. of 4 to 13.

Indicated Thermal Efficiency as Affected by Heat Load

It was found as a result of an extensive series of experiments with benzene–air mixtures (5) in the low heat load conditions, that optimum values for I.T.E. over a wide range of M.S. were obtained when spark timing was fixed at 20° in advance of t.d.c. and C.R. always adjusted for maximum power output as M.S. was varied. The relation between Opt. C.R. and M.S. thus obtained is given by graph A of Fig. 5, and the corresponding values of I.T.E. by graph B.
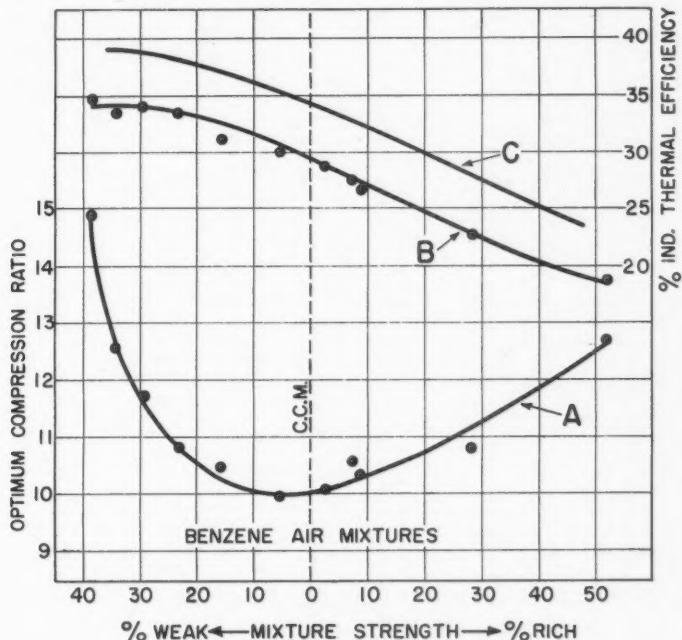
FIG. 5.   Heat load, effect on I.T.E.
C. I.T.E. with high heat load.
B. I.T.E. with low heat load.
A. Common base of optimum C.R.

Now by making use of the data given by the graphs of Fig. 4, the I.T.E. values for similar values of M.S. and C.R. as determined in the running conditions of the higher heat load can be obtained. These are given by graph C of the figure and it will be understood that the values of I.T.E. shown by graphs B and C are derived from the common basis of Opt. C.R. and M.S. as represented by graph A. The noteworthy feature of the experimental results is that thermal efficiency increased on increasing the temperature of the cycle. This anomalous result is attributed to the increase in inflammability of the benzene–air mixture due to the increase of heat load and the consequent addition of the heat of combustion of the benzene to the working fluid at more nearly constant volume, this effect being great enough to more than offset the adverse effect of increasing the temperature of the cycle.

Indicated Thermal Efficiencies Compared with Ideal Values

The relation between I.T.E. and C.R. is given by graph A of Fig. 6, for benzene–air mixtures used in conditions of the low heat load and with ignition timing fixed at 20° in advance of t.d.c. A single hot spark plug, C.F.R.-8, was used. There is shown a just measurable increase in I.T.E. for an increase of
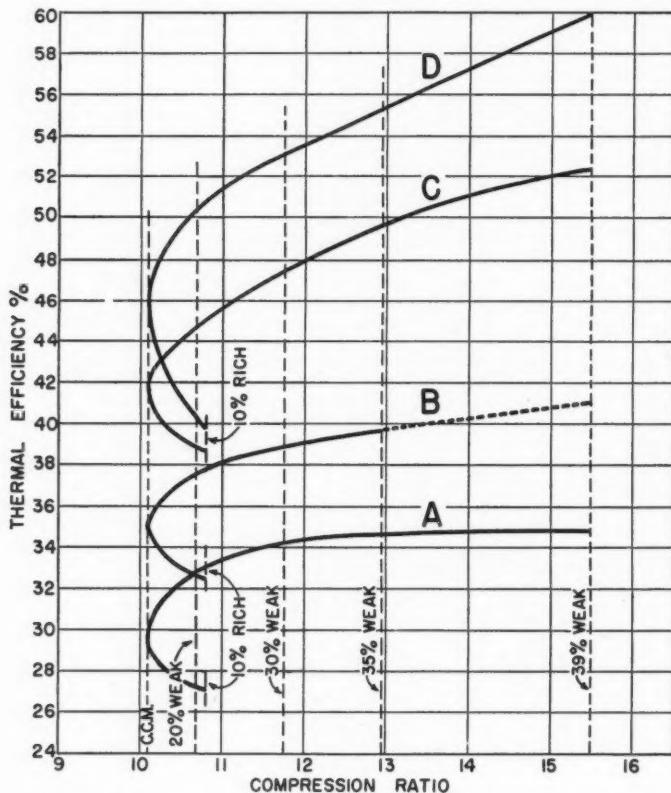

FIG. 6.   Observed indicated thermal efficiencies.
             Benzene–air mixtures compared with calculated ideal values.
             A. Observed, with low heat load.
             B. Observed, with higher heat load.
             C. Ideal, calculated by "Leah" method.
             D. Ideal, calculated by text book method (Pye).

C.R. from 13 to $15\frac{1}{2}$ and a decrease of M.S. from 35 to 39%. The small increase in I.T.E. in the circumstances is attributed to the slow burning of the benzene. Thus for example, the occurrence of maximum combustion pressure 2 to 3° earlier for a mixture 37.7% weak than for one 23.3% weak, Part XXII (5, p. 29, Table II), is attributed to combustion not having been complete at the

piston position at which it was indicated to have occurred. That is, the cycle was changing from constant volume to constant pressure.

The higher values for I.T.E., graph B, are from the data of Fig. 4 for the results of experiments made in the higher heat load conditions and are for the values of C.R. and M.S. for which graph A was obtained. Although two cooler spark plugs, at mid position on the heat scale, were used, the engine would run on weak mixtures for a short period without spark, graph B, Fig. 6. This igniting effect requires further investigation in view of the possibility that the benzene began to decompose to yield diphenyl and hydrogen at the gas temperatures attained at values of the C.R. higher than 13.

Graph C of the figure is for ideal values of thermal efficiency for benzene–air mixtures calculated by the method devised by Leah (7), and modified to allow for engine speed, cylinder dimension, and particular values of the initial temperature of compression. It is assumed however, as in theoretical calculations by others, that the heat of combustion of the benzene is added to the working fluid at constant volume.

Graph D is for ideal values of thermal efficiency as calculated by Pye (10, p. 181) with the use of the most reliable values for specific heats and dissociation available at the time. No allowance was included for engine speed and dimensions. The initial temperature of compression was taken as 212° F. and the calculations were based on a constant volume cycle.

The graphs of Fig. 6 illustrate the increasing rate of departure of real from ideal values of thermal efficiency, with decreasing concentration of benzene in mixtures with air and the consequential decreasing rate of burning of the benzene–air mixture. They show that deductions, based on the assumption that graphs for the variation of ideal and real values of thermal efficiency with compression ratio lie parallel though separated, as made by Pye (10, pp. 181–183) for example, and others, are not justified.

IV. NUCLEAR IGNITION AND THE ADVERSE EFFECT ON THERMAL EFFICIENCY

The adverse effect is exhibited by the graphs of Figs. 7, 8, and 9. These enable a comparison to be made of the values for I.T.E. determined when using pentane, hexane, and heptane in the running conditions required for nuclear ignition, with those determined when using benzene with similar values of C.R. and M.S. and with ignition necessarily by spark. The graphs of the three figures are lettered similarly and the references below will be made accordingly.

The A graphs, for the relation between C.R. and M.S., are of the W form always obtained when the paraffins are used in the conditions required for nuclear ignition. It differs characteristically from the U form obtained for benzene, with spark ignition even at relatively high values of C.R., as shown by graph A of Fig. 5.

The B graphs are for values of I.T.E. as determined for the paraffins when used at the values of M.S. and C.R. shown by the A graphs.

The C graphs are for values of I.T.E. determined when benzene was used at the values of C.R. and M.S. shown by the A graphs. The data for the C graphs

were obtained from the family of graphs, Fig. 4, and are extended into the weak mixture region, only until misfiring began.

It is to be remembered that the values given for benzene were determined in the higher heat load conditions in which an approach to a constant volume cycle was obtained for values of M.S. in the neighborhood of correct, and that the value of I.T.E. for any particular M.S. and the corresponding C.R., as taken from the graphs of Fig. 4, was always determined with optimum spark
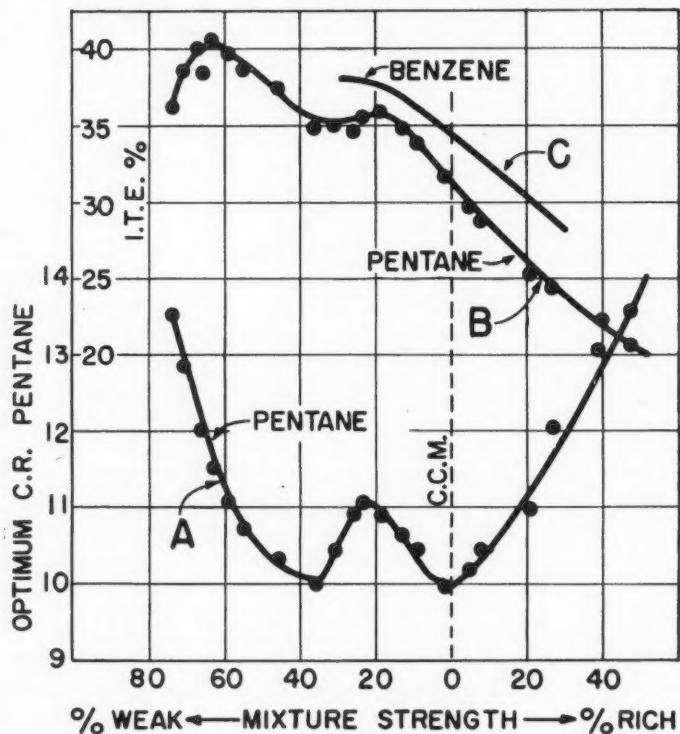

Fig. 7.   Comparable values of I.T.E.   Pentane with nuclear ignition.   Benzene with spark ignition.

timing. The data for the paraffins were obtained when using compression ratios required for nuclear ignition with values always adjusted for maximum power output, that is, to an optimum. The heat of combustion was always added, in the circumstances, to the working fluid at constant volume as illustrated by the indicator diagrams of Fig. 1.

The values for I.T.E. obtained in the circumstances were always lower for the paraffins than for benzene, as shown by the B and C graphs of Figs. 7, 8, and 9. The percentages by which they were lower were 7% for pentane and hexane and 8% for heptane when M.S. was 20% weak. At correct mixtures, I.T.E. for the three paraffins was approximately 10% lower than for benzene.
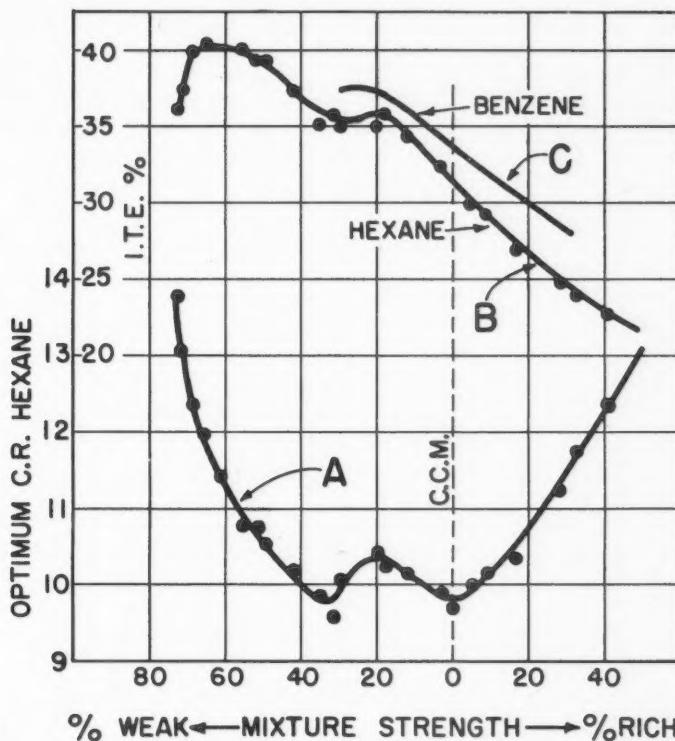
FIG. 8. Comparable values of I.T.E. Hexane with nuclear ignition. Benzene with spark ignition.

The extent to which relative values for I.T.E. were affected by the changes in running conditions that were required to obtain an approach to a constant volume cycle when using benzene may require some consideration.

The most important change was the increase in speed from 400 to 900 r.p.m. The effect on I.T.E. as measured over a higher speed range has been investigated by Ricardo for liquid fuels when used with spark ignition, and found to be negligible, as discussed by Pye (10, p. 205).

When using a paraffin with ignition by *compression* the increase of speed from 400 to 900 r.p.m. would, according to the nuclear theory, have the effect of extending two stage ignition into mixtures richer than 20% weak, with the consequence that I.T.E. for these would be lower than was determined at 400 r.p.m.

The jacket coolant was maintained at 100° F. for the experiments with the paraffins and at 140° F. for those with benzene. It was shown by experiments with town gas, described in Part XII of this series of papers, that the effect on I.T.E. of increasing the jacket coolant by 72° F. was nil. A larger increase of 211° F. led to a *decrease* of 2.5%.

The increase in the temperature of the air supply of from 50° F. to 140° F. for the benzene experiments would raise the temperature of the cycle and consequently be of adverse effect on thermal efficiency.

The increase in I.T.E. obtained on increasing charge density to "normal", when using a paraffin fuel, is discussed in Section VI and shown by the graphs of Fig. 10. An increase occurred when using the weak mixtures in which ignition and combustion occurred in two stages. These mixtures were leaner than any benzene–air mixtures that could be ignited by an electric spark and it was concluded that I.T.E. for benzene was not affected by charge density over the range of mixture strength ignitable by spark.
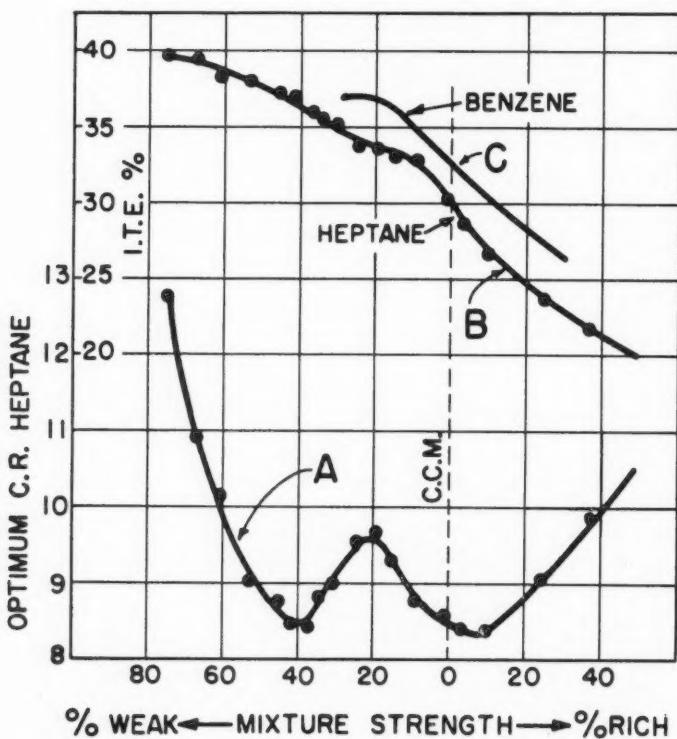
FIG. 9. Comparable values of I.T.E. Heptane with nuclear ignition. Benzene with spark ignition.

V. RESIDUAL PRODUCTS OF THE DECOMPOSITION OF PARAFFIN FUELS

It is shown by the diagrams of Fig. 1 that nuclear ignition of the paraffins used for the experiments occurs in a single stage with mixtures richer than approximately 20% weak. The quantity of very finely divided carbon derived

from the cracking of the paraffin would depend on charge density, M.S., C.R., engine speed, and the stability of the fuel molecules. As it would exist in a finely divided state, it would tend to be burned in the flame or to be carried out of the combustion chamber during the exhaust stroke. The amount of deposit remaining in the combustion chamber would then depend mainly on its retention by a film of lubricating oil.

When heptane was used as a fuel, with a charge density of 78% of normal, scattered particles of carbon appeared on the piston crown and patches of carbon on the blind plugs when M.S. was increased to be 20% weak. This was after the engine had run on still weaker mixtures and a brown color had been obtained only on the surfaces mentioned. On further increasing M.S. to the correct value, a very thin and patchy layer of carbon was seen on the piston crown and a nearly uniform layer on the cooler surfaces of the blind plugs. A further increase in the carbon residue was observed when over-rich mixtures were used, Part XXI (6, p. 245).

Observations of carbon residues made recently but with the lower charge density of 64% of normal disclosed that as before, carbon deposits on the piston crown became just visible with mixtures 20% weak, but there was little increase in their density as mixture strength was increased, C.R. always being adjusted to maintain maximum power output.

The engine was used recently for a series of experiments with extremely weak heptane–air mixtures extending over a period of several weeks. Consistent experimental results then ceased to be obtained and the engine was dismantled for inspection. All water cooled surfaces were found to be coated with globules of a resin-like substance varying in size to a maximum of about 1/64 in. in diameter. A similar deposit, but extremely thin, was found on the inlet valve. There was no deposit on the exhaust valve. These deposits could be wiped off easily. The deposits varied in color. They were dark brown on the water cooled surfaces, including the inner ends of the blank spark plugs. There was a similar color on the rim of the piston crown but it tended to turn reddish brown and then to a purplish brown as the center was approached. The deposits not exposed directly to flame tended to build up and become black and gummy. Those on uncovered screw threads of spark plug holes which were not sealed by the unthreaded ends of the blank spark plugs became so hard that a spark plug tap was required for their removal.

A black, very gummy deposit was found on the lands between piston rings and on the faces of the second and third compression rings which had become stuck in their grooves. The oil scraper ring had remained in good operating condition. All grooves of the compression rings were filled with the black gummy deposit. This had hardened to such an extent that the second and third rings could not be removed without being broken. It appeared that the deposits found below the crown of the piston were similar initially to those found in the combustion chamber but that they had become mixed with decomposed lubricating oil and had tended to accumulate and harden when not exposed to oxidizing conditions.

It is well known that aldehyde especially is a product of the combustion of weak mixtures in diesel engines and Webber (13), when discussing methods of maintaining pistons and rings in clean condition, mentions that synthetic resins formed from the aldehyde provide the binding for carbonaceous deposits.

VI. DISCUSSION

Reactions Prior to Ignition

Oxidation or decomposition reactions may occur prior to spark ignition in a carburetor engine, and experiments by others have been carried out in conditions such that oxidation reactions predominate. Thus jackets have been maintained at relatively high temperatures and heat added to the fuel–air mixtures in an attempt to reproduce the temperature conditions of maximum power output at the relatively low compression ratios required to avoid detonation when spark ignition is used. In these circumstances aldehyde is the first oxidation product formed in measurable quantity and its formation is accompanied by a minute proportion of peroxide. The peroxide has been assumed to be responsible in one way or another for the autoignition and the consequent "detonation" obtained on raising the compression ratio when fuels subject to that phenomenon are used. A "motored" engine without spark ignition is used frequently for these experiments.

It appears that Callendar and associates (1, pp. 27–28), 1926, were the first to use a motored engine to demonstrate the formation of aldehydes and peroxides in the temperature condition mentioned. Improved methods of experiment were used by Egerton and associates (2), 1935, in that by means of a sampling valve, the increase in the rates of formation of aldehyde and peroxide during compression were determined while the engine was developing power.

There was little if any publication of results of similar investigations until in recent years the possible effect of preflame reactions on the velocity of combustion in other than piston engines became of interest. Preflame reactions can however be studied most conveniently when using piston engines. Experiments made accordingly, but in temperature conditions suitable for the promotion of oxidation reactions, have been described recently by Retailliau, Ricards, and Jones (11), by Levedahl and Howard (8), and by Pastell (9). It is mentioned by Pastell that the form of the graph, Fig. 4, of his paper may be due to endothermic cracking reactions.

Method Used During Compression to Promote Decomposition Reactions Only

The method was devised to avoid surface oxidation of the fuel during compression and to make possible the use of paraffin fuels at compression ratios such that the temperatures and pressures attained by the end of compression would approach those of the end gas with ignition by spark. Autoignition would then, at a suitable high compression ratio, be initiated in some part of the whole charge instead of in some part of the end gas only.

Oxidation was avoided by the use of operating conditions required for an

exceptionally low heat load as described in Section I. The surface in the combustion chamber which, in the absence of a spark plug, would attain the maximum temperature was that of the exhaust valve. Its mean temperature was shown by separate experiments to be approximately 625° F. (329° C.) when the engine was running on autoignition, a correct heptane–air mixture, and the C.R. required for maximum power output. The temperature fell rapidly to 330° F. (165° C.) approximately as M.S. was reduced to 20% weak. The low heat load of the experiments was due in part to a reduction of charge density, generally to 64% of normal. This, in addition, had the effect of reducing the pressure due to autoignition to an extent that could be tolerated by the engine. Thus it was possible to measure the indicated thermal efficiency corresponding to the maximum power output for any ignitible mixture and to compare the values with those obtained when using a fuel such as benzene which did not decompose in the engine to provide material nuclei of ignition.

The Adverse Effect of Decomposition on Thermal Efficiency

The heat of compression would be insufficient, on the basis of published values for the "energy of activation", to decompose the whole of the fuel in a mixture even 20% weak to the extent required to produce finely divided carbon as nuclei of ignition. The values were obtained for vapors unmixed with air, contained in glass reactors, externally heated. They may not apply to engine conditions in which the vapor is mixed with air and heated rapidly by compression. It may however safely be assumed, in the absence of relevant data, that, as stated in Part XX (4, p. 39), decomposition of the fuel to the extent necessary to produce nuclei of ignition would occur in the part of the charge which had attained a higher than average temperature. That would be the part adjacent to the hot exhaust valve. It is not yet clear whether the rapid combustion which follows the nuclear ignition of this part of the charge is due to the consequent pressure wave or to a thermal process initiated by a relatively large volume of flame. The process of the nuclear ignition and subsequent combustion of the charge occurred in approximately 3° of crank revolution when a correct heptane–air mixture was used at a C.R. of 8.5, Fig. 1. That would be in 0.00125 sec., and a comparison of the values of I.T.E. obtained accordingly with those for the relatively slow burning benzene presents some difficulty. Thus we obtained a value of 31% for I.T.E., when using a correct benzene–air mixture at a C.R. of 7.0, and a heat load such that preignition did not occur (5, p. 33). Ricardo, using a heat load estimated to have been 40% greater, obtained 37% for the I.T.E. at a C.R. of 6.9, but could not use a higher value because of the onset of preignition (12, pp. 144–145). Furthermore it will be seen by reference to Fig. 6 that an increase of heat load from a relatively low value to the maximum used for the experiments with benzene described in this Part led to an increase in I.T.E. of from 29.5 to 35%, at a C.R. of 10. This increase was shown by experiment to be due to the heat of combustion of the benzene having been added to the working fluid at more nearly constant volume. It is to be noted here that the increase occurred in spite of the decrease that would be expected because of the higher temperature

of the cycle. The heat of combustion of the paraffin is shown by the indicator
diagrams of Fig. 1 to have been added to the working fluid at constant volume
for mixtures within the range correct to 20% weak. It may be concluded
therefore that higher values for I.T.E. than those observed would have been
obtained for benzene–air mixtures if it had been possible to use a higher heat
load without the onset of preignition. The result would be that a greater
adverse effect on thermal efficiency than that observed could then be attri-
buted to the heat absorbed by the decomposition reaction required for the
nuclear ignition of the paraffin–air mixtures. This, as shown by the B and C
graphs of Figs. 7, 8, and 9, accounted for the values of I.T.E. for the paraffins
being from 7 to 10% lower than those for benzene, in similar conditions of
M.S. and C.R.

The Nuclear Theory of Ignition

The theory was developed, as described in Part IV (3), to account for the
autoignition of the end gas in spark ignition carburetor engines. It was there-
fore applied only to fuel–air mixtures richer than 20% weak because spark
ignition tends to be ineffective as mixture strength is further reduced. Auto-
ignition with mixtures richer than 20% weak was attributed, according to the
theory, to the igniting effect of finely divided carbon derived from the cracking
of the fuel at the temperature and pressures attained by the end gas, and
residues of the carbon always appeared on the piston crown.

It is significant that, when using mixtures leaner than 20% weak, formalde-
hyde was detectable in the exhaust and residues of a resinous nature appeared
on the piston crown, Part XXI (6, pp. 246–247), and that, after a long period
of running on weak mixtures, residues which appeared to be a mixture of resins
and carbon had the effect of sticking piston rings firmly in their grooves,
Section V.

The surfaces in the combustion chamber of the C.F.R.-F2 engine do not
attain temperatures required for the oxidation of the paraffins to aldehyde in
the low heat load conditions of the experiments even when correct mixtures
are used. This statement is based on temperature measurements which will
be described in a subsequent Part. However, on decreasing M.S. and raising
C.R. to maintain optimum power output, there is a further decrease in heat
load, which depends mainly on the heat of combustion; thus surface tempera-
tures decrease while the temperature of the charge increases. The aldehyde
always present in the products of the combustion of weak mixtures must then
have been formed on the carbon nuclei present in the charge as a result of the
cracking of the paraffin. The compressed mixture may then contain nuclei of
finely divided carbon and nuclei composed of a mixture of resins and carbon,
which differ in degree of inflammability. This difference affords an explanation
for the occurrence of two-stage ignition in mixtures leaner than 20% weak, in
the conditions of the experiments described in this Part.

This extension of the nuclear theory of ignition, although regarded at present
as a working hypothesis, appears to afford an explanation for the characteristics
of the two-stage ignition of mixtures leaner than 20% weak.

Nuclear Ignition and the Lower Limit of Inflammability

The indicator diagrams of Fig. 1 show that the nuclear ignition of heptane, taken as a typical paraffin, occurred in a single stage when mixtures with air richer than 20% weak were used. It is indicated by experiments described earlier that the nuclei of ignition were those of finely divided carbon. Ignition began to occur in two stages when weaker mixtures were used. It will be seen by reference to the graphs of Figs. 7 to 9 that this double igniting effect continued to be effective until the paraffin–air mixtures were from 70 to 80% weak. This was not the limit. In other experiments, Part XXI (6, p. 244) with heptane as the fuel, nuclear ignition continued, as C.R. was always raised to an optimum value as M.S. was diminished until it became 93% weak. The air–fuel ratio was then 220 : 1 by weight and the Opt. C.R. 22.8. The power developed was not sufficient to run the engine at the speed of the experiments, 400 r.p.m., and the deficiency in power was supplied from the dynamometer used as a motor. Heptane was used for these experiments because it decomposes more readily than hexane or pentane to supply nuclei of ignition.

The experimental results show that the enormous extension of the lower limit of inflammability of the paraffin–air mixtures was not due fundamentally to the high temperatures and pressures attained on increasing C.R. Thus it occurred solely when using the fuels which could be decomposed to provide material nuclei.

Characteristics of Two Stage Nuclear Ignition; Mixtures Leaner
Than 20% Weak

The mixture range 20 to 40% weak was marked by the advent of two-stage ignition, the occurrence of formaldehyde in the exhaust, the appearance of residues of combustion which appeared to be mixtures of resins and carbon, a decrease in the C.R. required to maintain optimum power output, and a tendency for I.T.E. to remain constant. A nearly constant value was obtained when using hexane and pentane and an approach to such a value when using heptane, see Fig. 3. The nearly constant value for I.T.E. can be accounted for, as mentioned earlier, by the increase due to decreasing M.S. being offset by the decrease due to decreasing values of Opt. C.R. The decrease in Opt. C.R. is attributed, according to the extension of the nuclear theory, to the compressed charge containing two types of nuclei, namely, those of finely divided carbon and others consisting of mixtures of carbon and resins. The latter being the more inflammable would initiate a first stage of ignition which would cause and be followed immediately by a second stage depending on the less inflammable nuclei of finely divided carbon.

The increase of C.R. required to maintain optimum power output when using mixtures leaner than 40% weak is regarded as being required to maintain a necessary first stage of ignition. The first stage, on this basis, must be considered as a "primer" for the second stage.

The values of I.T.E. for mixtures leaner than 40% weak rose slowly in relation to the increase of C.R. required to maintain optimum power output. A maximum value of 40% for I.T.E. was obtained when mixtures were 65%

weak. There was then a rapid decrease in I.T.E. as mixtures leaner than 65% weak were used, although C.R. was raised rapidly in order to maintain an optimum value. Thus I.T.E. had fallen to 34% and Opt. C.R. had risen to 15.5 when the mixture became 80% weak.

The relatively low values for maximum I.T.E. obtained in the low heat load conditions of the experiments can be explained as follows: The heat due to combustion of the fuel decreases proportionally to the decrease in M.S., with the consequence that the mean temperatures of the surfaces in the combustion chamber decrease and an increasing proportion of the heat of compression is absorbed by them. An abnormal increase in Opt. C.R. is then required to raise the temperature of the gaseous charge to that required for decomposition of the paraffin to the extent required for the provision of nuclei of ignition. The *quantity* of heat available during compression can however be increased by increasing charge density, without increasing the temperature, if compression ratio remains unchanged. Thus an increased proportion of the
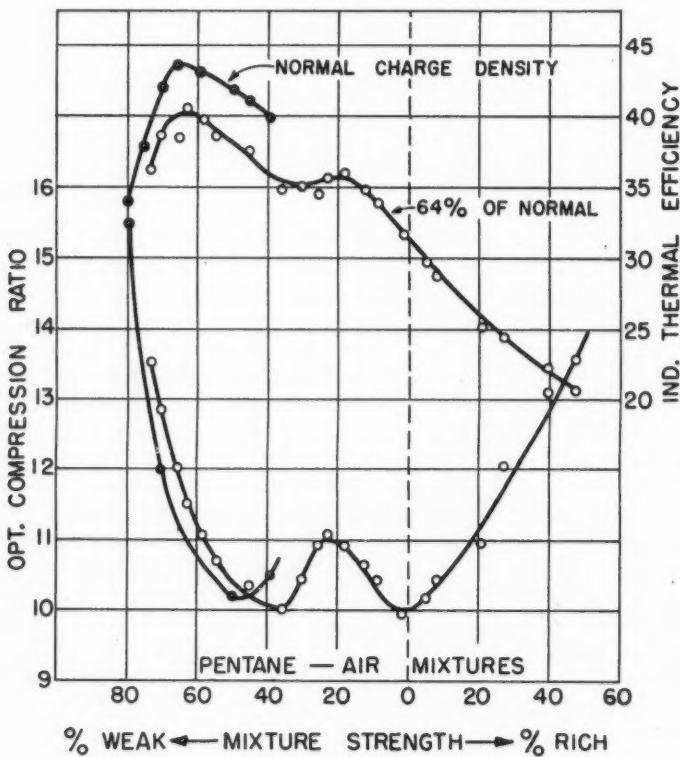
FIG. 10.   Effect of increase of charge density to increase I.T.E.
● Normal charge density.
○ 64% of normal.

heat of compression would be available for the decomposition reaction and for conversion into power with a corresponding increase in I.T.E.

An experiment was tried accordingly with a charge density of "normal", obtained by using the standard C.F.R. carburetor fitted with a 9/16 in. diameter venturi instead of the choke tube used to obtain 64% of normal charge density. It is estimated that an increase of charge density of 33% was obtained. The other running conditions were not changed, that is, engine speed was maintained at 400 r.p.m., the jacket coolant at 100° F., and the air supply at 50° F. Beginning with a mixture 80% weak, it could be increased to 40% weak before the occurrence of an intolerable intensity of knocking combustion. The results of the experiments are exhibited by the graphs of Fig. 10. They show that maximum I.T.E. increased by approximately 9% on increasing the charge density while the corresponding Opt. C.R. decreased from 11.7 to 11.1, and it appears that with the greater available quantity of heat, the increase of I.T.E. was obtained with a lower compression temperature.

CONCLUSION

The method used for the experiments with the paraffins has made possible the investigation of the gas phase reactions required for ignition by compression and the nature of these as affected by mixture strength. The experimental work is regarded as being of a preliminary nature. Further data relating to two-stage ignition, surface temperatures, and the mechanism of decomposition of fuels in engine conditions are required for a more complete understanding of the fundamentals of combustion as it occurs in engines.

ACKNOWLEDGMENTS

REFERENCES

1. CALLENDAR, H. L., KING, R. O., MARDLES, E. W. J., STERN, W. J., and FOWLER, N. R. Aeronaut. Research Comm. Repts. and Mem. No. 1062. 1926.
2. EGERTON, A., SMITH, F. L., and UBBELOHDE, A. R. Trans. Roy. Soc.(London), A, 234: 433–521. 1935.
3. KING, R. O. Can. J. Research, F, 26: 228–240. 1948.
4. KING, R. O. and ALLAN, A. B. Can. J. Technol. 30: 44–60. 1952.
5. KING, R. O. and ALLAN, A. B. Can. J. Technol. 32: 22–48. 1954.
6. KING, R. O., DURAND, E. J., ALLAN, A. B., HANSEN, E. J. T., and BOWER, V. E. Can. J. Technol. 30: 222–257. 1952.
7. LEAH, A. S. Engineering, 168: 665–668. 1949.
8. LEVEDAHL, W. J. and HOWARD, F. L. J. Research Natl. Bur. Standards, 46: 301–309. 1951.
9. PASTELL, D. L. Trans. Soc. Automotive Engrs. 4: 571–587. 1950.
10. PYE, D. R. The internal combustion engine. 2nd ed. Oxford University Press, London. 1937.
11. RETAILLIAU, E. R., RICARDS, H. A., JR., and JONES, M. C. K. Trans. Soc. Automotive Engrs. 4: 438–454. 1950.
12. RICARDO, H. R. Proc. Inst. Automobile Engrs. (London), 18: Part 1. 1923–1924.
13. WEBBER, M. W. Gas and Oil Power, 48: 223–225. 1953.

A PORTABLE ELECTRIC VELOMETER FOR LOW VELOCITY LIQUIDS[1]

BY A. D. MISENER

ABSTRACT

An electric instrument is described which is capable of measuring the flow velocities of liquids up to four miles per hour with an accuracy of better than 0.1 m.p.h. The absolute accuracy improves at lower velocities. The instrument described is self-contained and portable, suitable for study of stream velocities, erosion currents, ground runoff, etc. It may be readily adapted to become a recording velometer for any liquid, either in pipes or open channels. Its operation is not affected by sediments and suspended solids carried by the liquids.

INTRODUCTION

The devices at present used to measure the flow of liquids, such as orifice plates, venturi meters, and mechanical meters, are all inaccurate at lower rates of flow and become practically useless somewhere in the range below one mile per hour. To provide accurate flow measurements in the region of low velocities it was thought that use could be made of the fact that the flowing liquid would carry away heat supplied to a "detector" immersed in it. If the flow of liquid was slow, heat would be taken away slowly and, with a constant rate of supply, the temperature of the detector would rise until it was considerably above that of the liquid. For more rapid flow, the equilibrium between the heat input and heat loss to the fluid would be reached at a lower detector temperature.

This principle is similar to that employed in the hot-wire anemometer so widely used in meteorological observations in air velocities. The practical difference between the two cases comes from the fact that a liquid such as water flowing past a heated detector will take the heat away about 1000 times as rapidly as would air at the same velocity. A liquid velometer must therefore have a very large volume to area ratio and a sensitive temperature detector or else use an unreasonable amount of heat energy.

The theory of heat transfer from a heat source to a liquid flowing past it is undeveloped past the empirical stage. So many factors, shape, size, aspect of the heater, thermal diffusivity, viscosity, and velocity of the fluid, are interrelated in a variety of ways that the numerical values for the quantity of heat transferred must be determined for each individual case. For a particular detector, heated at a constant rate in a given liquid, general considerations predict that the velocity of flow (V) should be related to the equilibrium temperature difference between heater and liquid (ΔT) by the relation

$$V = C/(\Delta T)^2$$

where C is a constant involving all the factors mentioned above as well as the value of the constant heat input.

Preliminary experiments showed that this relation held over the range of

velocities anticipated and therefore that the detector would have a good absolute accuracy at flow velocities near zero. At higher velocities ΔT would be less and its determination therefore less accurate, but the resulting uncertainty in V would also represent a smaller percentage error. By constructing detectors with different values for C it should be possible to vary the range of velocities (V) which could be measured and still maintain sufficient accuracy with a single measuring circuit.

THE DETECTOR UNIT

Several different arrangements of temperature sensitive detectors and heaters were devised which would fulfill the requirements of small heat capacity, rapid and sensitive response to flow variations, and low power consumption. The arrangement finally selected is shown in Fig. 1, and a photograph of a disassembled unit in Fig. 2.
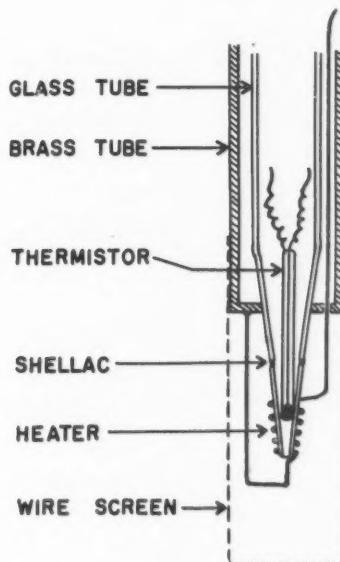
FIG. 1.   Diagram of the detector unit.

The temperature sensitive element is a small bead thermistor (Western Electric Type 6014A) with a resistance of approximately 10^5 ohms at 25° C., which is encased in a thin-walled glass tube. The heater coil is wound on a second thin-walled glass tube which is pushed over the thermistor and attached to it with shellac. This assembly is mounted in a sturdy brass tube through which the electrical leads from thermistor and heater are taken to terminals mounted on a handle at the top.

For protection against damage, a coarse wire screen surrounds the thermistor and heater and is soldered to the lower end of the brass tube. This tube may
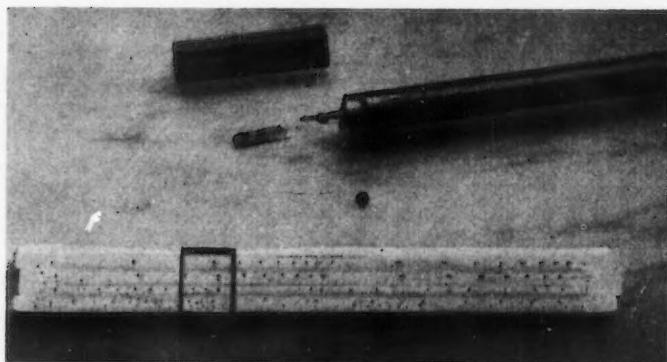
FIG. 2.   The detector unit disassembled to show components.

be of any convenient length and is marked off in inches to serve as a depth gauge. Because of the high resistance of the thermistor and adjustments available in the heater circuit (to be described later) it is possible to connect the leads at the top of the detector tube to the rest of the apparatus by means of an ordinary four-pronged socket.

CALIBRATION OF DETECTOR UNIT

The detector unit was mounted so that it could be moved at a known velocity in a large thermostatically controlled water tank. Baffles were placed
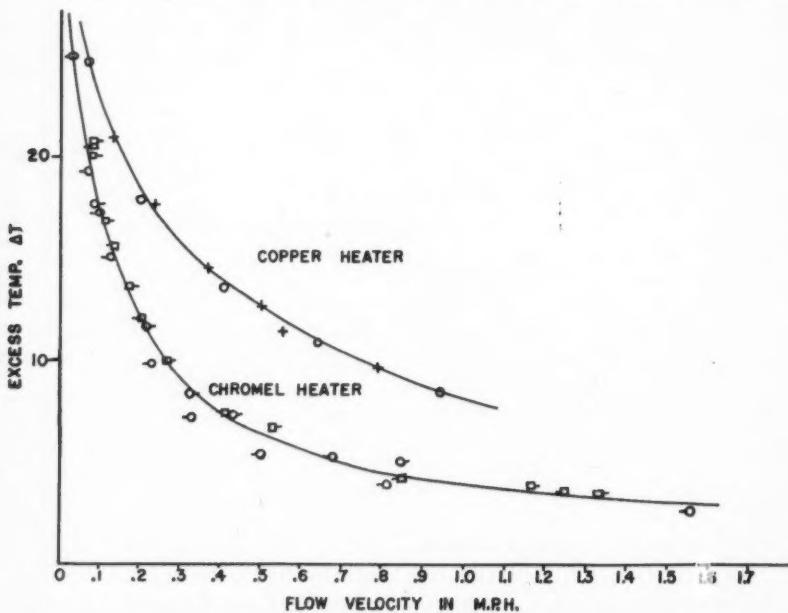
FIG. 3.   Calibration curves; two different detector units in water.

in the tank to prevent the water from moving with the detector. Because of the rapidity of response, only one or two circuits through the tank were required to establish a reading so the stirring of the water was negligible.

With a constant current supplied to the heater the excess temperature above tank temperature was recorded as a function of the velocity. Typical curves are shown in Fig. 3. The actual readings taken were, of course, thermistor resistance and velocity; the resistance readings were converted to temperature by the previously obtained calibration curve for the thermistor used. The temperature–resistance relation of this particular thermistor is nearly linear (to within 0.05° F.) over the temperature range 35° F. to 65° F., and so the curve of Fig. 3 is sufficiently accurate for many starting temperatures. If the temperature–resistance curve departs significantly from a straight line, or if
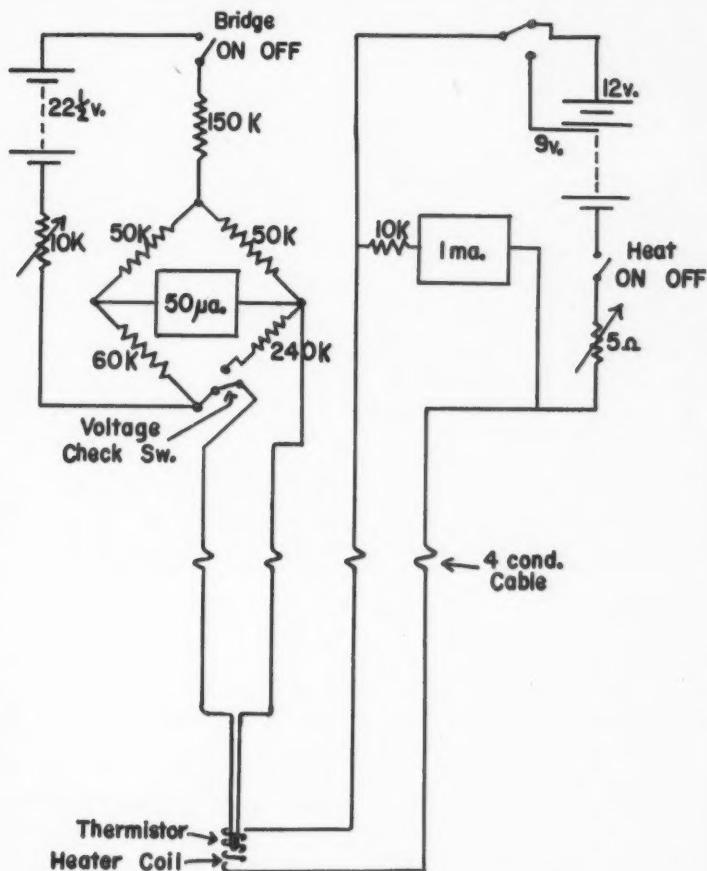
FIG. 4. Circuit diagram for the indicating and control unit.

the liquid to be measured is at unusually high or low temperatures, calibration of the detector unit at appropriate starting temperatures would have to be made.

INDICATING AND CONTROL UNIT

The battery power supply, adjusting circuits, and indicating meters are mounted together and connected to the detector unit by a convenient length of four-conductor cable. These circuits are shown in Fig. 4 and a photograph of the unit in Fig. 5. The heater supply voltage may be set at either of two values to provide two different ranges of sensitivity with respect to flow velocity.
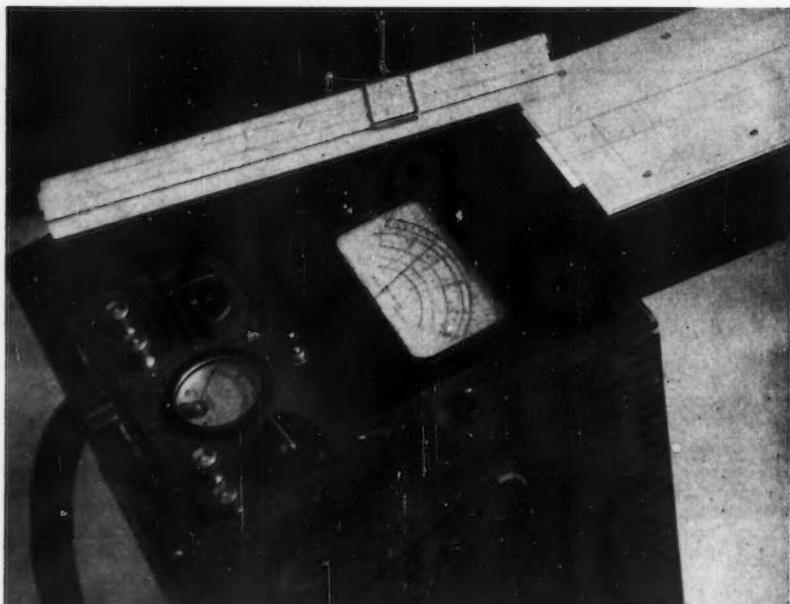
FIG. 5.   The indicating and control unit. Switches and meters on top of box which contains batteries and slide rule for detector unit (B) mounted on lid.

The thermistor bridge circuit is provided with a voltage check switch which removes the thermistor and introduces a known resistance into the bridge circuit. The bridge supply voltage may then be adjusted to give a standard bridge current as indicated by the microammeter.

For a particular detector unit and a given bridge current, the variation of resistance of the thermistor as its temperature is changed will produce a variation of current through the meter. Because of the high resistance of the thermistor this current change will be nearly proportional to the temperature change. It is therefore possible to convert meter readings directly to temperatures without the operations of balancing a bridge, etc. A typical conversion graph is shown in Fig. 6.

The three calibration curves, temperature vs. resistance of the thermistor, velocity vs. thermistor resistance, and thermistor resistance vs. meter reading, may be combined in a variety of ways to give a convenient method of rapidly determining velocity from meter readings. Any such combined "calibration curve" is valid for only a particular detector unit and, strictly, for one temperature of liquid. However, if the two conditions mentioned above are satisfied, viz. nearly linear temperature vs. resistance and high thermistor resistance, the calibration data may be combined into a slide rule which will connect meter readings to flow velocities for a wide range of starting temperatures.
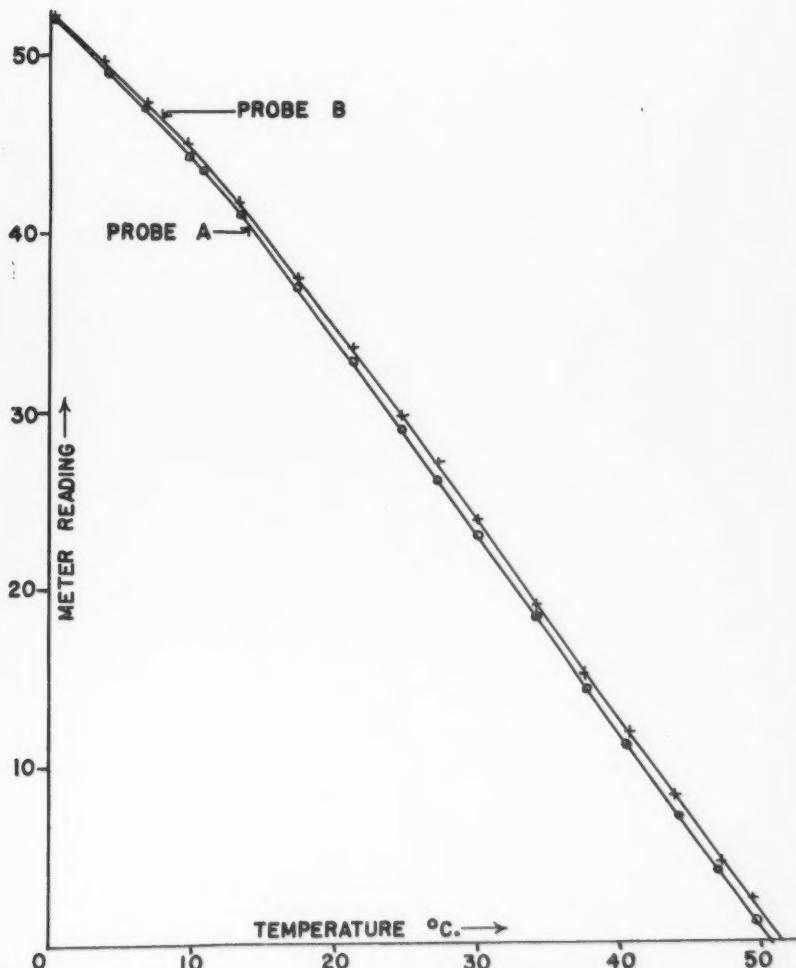
FIG. 6. Conversion graph of meter readings into temperature. Probe *A* refers to a detector with a copper heater. Probe *B* refers to a detector with a chromel heater.

Such a slide rule for a particular detector unit is shown mounted on the lid of the indicating unit in Fig. 5 and a copy of it in Fig. 7.

METHOD OF OPERATION

A detector unit is calibrated in the liquid it will be used to measure. This calibration is carried out using the particular heater voltages available in the indicating and control unit. The calibration data are combined in a slide rule to be used for that particular detector unit with that particular liquid. The same detector unit may be calibrated for a number of different liquids and appropriate slide rules constructed for each. The same detector unit may be
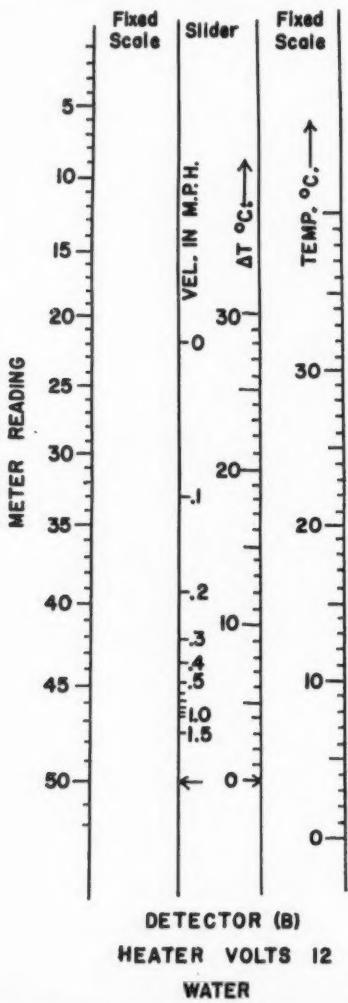
FIG. 7. Slide rule combining the various calibration curves for detector. (B) used in water.

calibrated in the same liquid with a number of different heater voltages, thus providing different ranges of sensitivity to flow. For all detector units provided with their appropriate slide rules the same indicating and control unit is used.

The detector unit is connected to the indicator unit with no power supplied to the heater element (heat switch off, Fig. 4). The bridge voltage check switch is closed and the rheostat adjusted till the microammeter indicates the correct bridge current. (This current is recorded on the face of the meter and is selected when constructing the indicating unit so that suitable meter readings will be obtained with the thermistors to be used as detectors.) The voltage check switch is changed to include the thermistor in the bridge circuit, and the detector unit immersed in the flowing liquid. The bridge meter reading will now indicate the temperature of the liquid. This may be read off from the fixed part of the slide rule. For example, if the detector unit for which Fig. 7 records the calibration data gave a meter reading of 50 when immersed in the fluid the temperature of the fluid was 3.5° C. The zero of the slider of the slide rule is now set at this value of meter reading and temperature.

Next the heater is switched on and if necessary the rheostat in the heater circuit adjusted until the current is the same as that used during calibration of the detector unit. The bridge meter reading is now taken and converted directly into liquid velocity by reading from the slide rule. For example with the setting shown in Fig. 7, a meter reading of 40 indicates a velocity of water of 0.22 m.p.h.

DISCUSSION

In this investigation no attempt was made to calibrate detector units for liquids other than water but there seems to be no reason why such units could not be constructed. The curves of Fig. 3 show how the sensitivity and range of detector units vary with their construction and it is probable that suitable choice of components, particularly the area to volume ratio of the heater–thermistor combination, would allow construction of a set of detector units covering a wide range of velocities. In one preliminary test, the application of a layer of thermally insulating shellac over the entire unit extended the usable range up to approximately 4.0 m.p.h. The electric velometer was more sensitive than the device used for determining the flow rate so these tests could not be used for calibration purposes.

The prototype instrument here described was field tested in the Thames and Medway Rivers and was found to give satisfactory records of the variation of flow velocity with depth at a series of locations taken across the rivers. Its accuracy was not affected by the silt and mud carried by the water. When occasional leaves or weeds clogged the protecting wire screen the sudden change of meter reading gave immediate indication of the trouble and the detector unit was simply cleaned off and resubmerged.

NOTE

CRYSTALLIZATION OF MILLIGRAM QUANTITIES OF ORGANIC COMPOUNDS

By George F Wright

The equipment used in organic chemical research is scaled principally to the macro size. While numerous devices have been reported for manipulation of milligram quantities, for the most part they are time-consuming in use and are not of general applicability. There is a need for simple apparatus with which 1–100 mgm. of material may be handled with the facility which has come during more than a century because of the present design of macroware. In the present report a device for crystallization of small amounts of material is described. The use of this apparatus precludes losses by evaporation of simple or mixed solvents and by evaporation from filter paper or from decolorizing adsorbent. Furthermore the use of this crystallizing tube facilitates the separation of a mixture of substances without appreciable loss of any part of the mixture.

The device is an elaboration of a side-arm test tube described for crystallization previously (1). The improved tubes are constructed from pyrex test tubes 100 × 15 mm., 75 × 12 mm., and 75 × 10 mm. O.D. The tube of intermediate size is shown in Fig. 1. During construction a bulge is formed in the tube. Then two diametrically opposed arms are attached at the bulge and the juncture of one arm is swelled into a trough shown at A. This construction ensures against contamination of the cork stopper used for closure of the top of the tube. It is convenient, though not necessary, to engrave the body of the tube into 0.25 or 0.5 ml. divisions for measurement of solvent or solution volume. The calibration is most useful when a mixed solvent is used for crystallization.

The tube is equipped for crystallization by insertion into the side-arms of long-staple cotton wool (previously ether-extracted for removal of fats) compressed into plugs 3–4 mm. long. The plug in the side-arm attached to the trough must be installed with care, especially when a finely-divided contaminant or decolorizing adsorbent is present. This plug is installed in the simplest side-arm, C, by compression between two rods inserted through the inlet and exit arms. Some skill is required in order that this plug shall not be dislodged by too much air pressure during the filtration through it. The alternative construction, E, obviates this difficulty. Its plug is tamped, via side-arm B, between the constriction and the notched depression G. The same loading is used in the side-arm shown at F (capillary tubing butt-sealed to 6 mm. tubing) except that a small filter paper may be inserted before the cotton plug is installed. Each of these filtering devices will retain the sediment or decolorizer which ordinarily is removed by filtration through a paper cone. After the filtering plug is installed the opposite side-arm is equipped with a cotton plug which serves only to act as a barrier in the event of sudden ebullition while
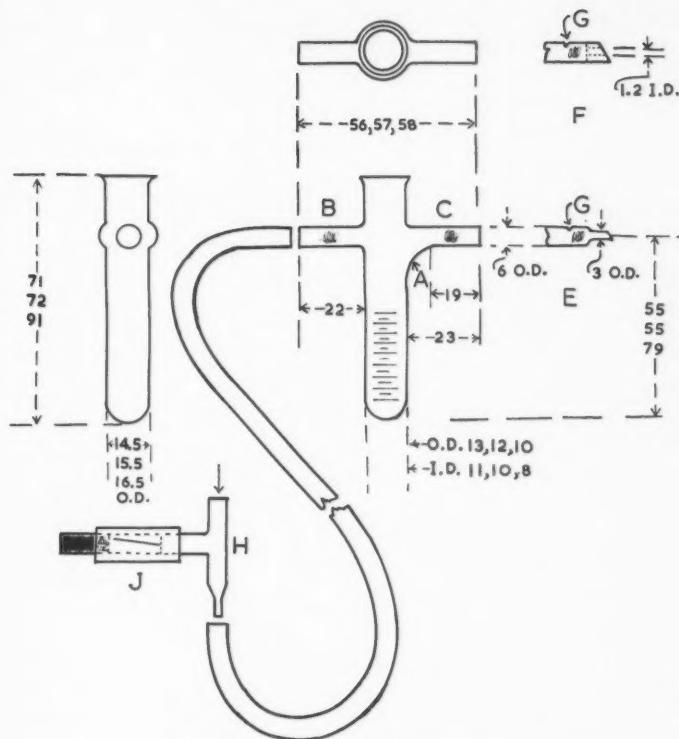
Fig. 1. Dimensions in millimeters.

the substance is being dissolved. A 3-ft. length of 1/8 rubber tubing is then attached to this barrier-plugged air inlet side-arm.

Into the tube that is equipped in this manner is placed the substance to be extracted or dissolved. Some solvent, together with a boiling chip is added and the corked tube is heated either with a liquid bath or a small bunsen burner. Any tendency toward "bumping" is alleviated by proper installation of the cotton plugs which act as vapor blocks preventing sudden ebullition. Additional solvent is added until further dissolution does not occur; if clarification is necessary some decolorizing adsorbent may be added after slight cooling. The hot solution is then filtered through the side-arm *C*, *E*, or *F* by aid of mild air pressure from the lungs through the attached rubber tubing; care is taken that the tube is inclined only enough that trough *A* is filled. Finally the tube is rinsed with a few drops of heated solvent which is expelled through the plug.

Sometimes the application of air pressure from the lungs becomes onerous because of slow filtration. If, in this event, a compressed air source is available, it may be utilized by attachment of the T-tube, *H*, with a bunsen release valve (*J* comprising a slit rubber tube). The "blow-tube" of the crystallizing appara-

tus may be inserted over the constricted end of this simple pressure regulator in order to dispense with the use of lung air-pressure.

It is obvious that loss of either material or solvent is minimized by this method of crystallization. The separation of a mixture is thus facilitated, especially if the double side-arm tube is used as a receiver during vacuum filtration to remove the crystal crop. The filtrate may then be evaporated in situ either by air stream or under reduced pressure (using a capillary tube of 0.1 mm. I.D. at the exit side-arm). The residue is available for a subsequent crystallization.

1. WRIGHT, G. F.   Can. J. Research, B, 17: 302.   1939.

DEPARTMENT OF CHEMISTRY,
UNIVERSITY OF TORONTO,
TORONTO, ONTARIO.

CONTENTS OF VOLUME 32

253

CORRECTIONS

Page 23. In line 1, paragraph 2, "experiment" should read "experiments".

Page 34. At the end of the first line and beginning of the second, "Fig. 9" should read "Fig. 10".

Page 35. In the caption of Fig. 12, under c and d, "3.0% weak" and "24.6% weak" should read "3.0% rich" and "24.6% rich", respectively.

Notes to Contributors

Manuscripts

(i) *General.* Manuscripts should be typewritten, double spaced, on paper $8\frac{1}{2} \times 11$ in. **The original and one copy are to be submitted.** Tables (each typed on a separate sheet) and captions for the figures should be placed at the end of the manuscript. Every sheet of the manuscript should be numbered.

Style, arrangement, spelling, and abbreviations should conform to the usage of this journal. Names of all simple compounds, rather than their formulas, should be used in the text. Greek letters or unusual signs should be written plainly or explained by marginal notes. Superscripts and subscripts must be legible and carefully placed.

Manuscripts should be carefully checked before they are submitted; authors will be charged for changes made in the proof that are considered excessive.

(ii) *Abstract.* An abstract of not more than about 200 words, indicating the scope of the work and the principal findings, is required, except in Notes.

(iii) *References.* References should be listed **alphabetically by authors' names**, numbered, and typed after the text. The form of the citations should be that used in this journal; in references to papers in periodicals, inclusive page numbers should be given but titles should not. All citations should be checked with the original articles and each one referred to in the text by the key number.

(iv) *Tables.* Tables should be numbered in roman numerals and each table referred to in the text. Titles should always be given but should be brief; column headings should be brief and descriptive matter in the tables confined to a minimum. Numerous small tables should be avoided.

Illustrations

(i) *General.* All figures (including each figure of the plates) should be numbered consecutively from 1 up, in arabic numerals, and each figure referred to in the text. The author's name, title of the paper, and figure number should be written in the lower left corner of the sheets on which the illustrations appear. Captions should not be written on the illustrations (see Manuscript (i)).

(ii) *Line Drawings.* Drawings should be carefully made with India ink on white drawing paper, blue tracing linen, or co-ordinate paper ruled in blue only; any co-ordinate lines that are to appear in the reproduction should be ruled in black ink. Paper ruled in green, yellow, or red should not be used unless it is desired to have all the co-ordinate lines show. All lines should be of sufficient thickness to reproduce well. Decimal points, periods, and stippled dots should be solid black circles large enough to be reduced if necessary. Letters and numerals should be neatly made, preferably with a stencil (**do NOT use typewriting**), and be of such size that the smallest lettering will be not less than 1 mm. high when reproduced in a cut 3 in. wide.

Many drawings are made too large; originals should not be more than 2 or 3 times the size of the desired reproduction. In large drawings or groups of drawings the ratio of height to width should conform to that of a journal page but the height should be adjusted to make allowance for the caption.

The original drawings and one set of clear copies (e.g. small photographs) are to be submitted.

(iii) *Photographs.* Prints should be made on glossy paper, with strong contrasts. They should be trimmed so that essential features only are shown and mounted carefully, with rubber cement, on white cardboard.

As many photographs as possible should be mounted together (with a **very** small space between each photo) to reduce the number of cuts required. Full use of the space available should be made and the ratio of height to width should correspond to that of a journal page; however, allowance must be made for the captions. Photographs or groups of photographs should not be more than 2 or 3 times the size of the desired reproduction.

Photographs are to be submitted in duplicate; if they are to be reproduced in groups one set should be mounted, the duplicate set unmounted.

Reprints

A total of 50 reprints of each paper, without covers, are supplied free. Additional reprints, with or without covers, may be purchased.

Charges for reprints are based on the number of printed pages, which may be calculated approximately by multiplying by 0.6 the number of manuscript pages (double-spaced typewritten sheets, $8\frac{1}{2}$ in. $\times 11$ in.) and making allowance for space occupied by line drawings and halftones (not inserts). The cost per page is given on the reprint requisition which accompanies the galley.

Any reprints required in addition to those requested on the author's reprint requisition form must be ordered officially as soon as the paper has been accepted for publication.

Contents